



Republic of Iraq

Ministry of Higher Education & Scientific Research

University of Kerbala

College of Engineering

Civil Engineering Department

Characterizing Sustainable Grout for Infrastructure Units

A Thesis Submitted to the Council of College of the Engineering/University
of Kerbala in Partial Fulfillment of the Requirements for the Master Degree
in Infrastructure Engineering

Written by:

Huda Mohammed Hasan

Supervised by:

Asst.Prof . Laith Mohammed Ridha Mahmmod

Asst. Prof. Dr. Muhammad Abdulredha

February 2023

Rajab 1444

بِسْمِ اللَّهِ الرَّحْمَنِ الرَّحِيمِ

﴿ يَرْفَعِ اللَّهُ الَّذِينَ آمَنُوا مِنْكُمْ وَالَّذِينَ
أُوتُوا الْعِلْمَ دَرَجَاتٍ وَاللَّهُ بِمَا تَعْمَلُونَ

خَيْرٌ ﴾

صدق الله العلي العظيم

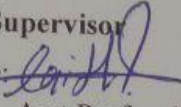
سورة المجادلة

آيه ١١

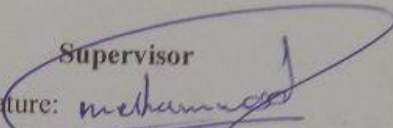
Examination committee certification

We certify that we have read the thesis entitled "Characterizing Sustainable Grout for Infrastructure Units," and as an examining committee, we examined the student "Huda Mohammed Hasan" in its content and in what is connected with it and that, in our opinion it is adequate as a thesis for the degree of Master of Science in Civil Engineering.

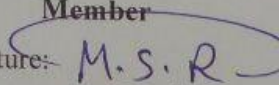
Supervisor

Signature: 
Name: Asst. Prof. Laith
Mohammed Ridha
Mahmoud
Date: 12/2/2023

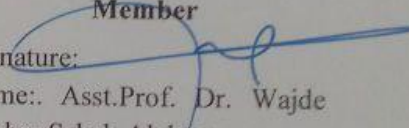
Supervisor

Signature: 
Name: Asst. Prof. Dr.
Muhammed Abdulredha
Date: 12/2/2023

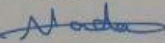
Member

Signature: 
Name: Asst. Prof. Dr.
Mushtaq Sadiq Radhi
Date: 12/2/2023

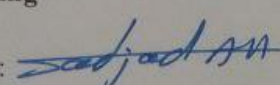
Member

Signature: 
Name: Asst. Prof. Dr. Wajde
Shober Saheb Alyhya
Date: 12/2/2023

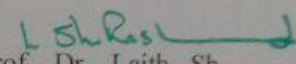
Chairman

Signature: 
Name: Prof. Dr. Nada
Mahdi Fawzi Aljalawi
Date: 12/2/2023

Approval of Head of Civil Engineering

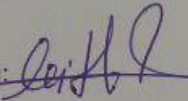
Signature: 
Name: Prof. Dr. Sadjad
Amer Hemzah
Date: /2/2023

Approval of Dean of the College of Engineering

Signature: 
Name: prof. Dr. Laith Sh.
Rasheed
Date: /2/2023

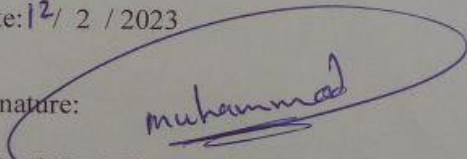
Supervisor certificate

We certify that the thesis entitled “**Characterizing Sustainable Grout for Infrastructure Units**” was prepared by **Huda Mohammed Hasan** under our supervision at the Department of Civil Engineering, Faculty of Engineering, The University of Kerbala as a partial of the fulfilment of the requirements for the Degree of Master of Science in Civil Engineering.

Signature: 

Asst.Prof .Laith Mohammed Ridha
Mahmmod

Date: 12/ 2 / 2023

Signature: 

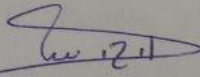
Asst. Prof. Dr. Muhammad Abdulredha

Date: / 2 / 2023

Linguistic certificate

I certify that the thesis entitled "**Characterizing Sustainable Grout for Infrastructure Units**" which has been submitted by **Huda Mohammed Hasan**, has been proofread, and its language has been amended to meet the English style.

Signature:



Name: Prof. Azhar Hassan Sallomi

Date: 13 / 2 / 2023

Abstract

Cement grout is widely used for the structural rehabilitation of concrete components, trenches, mine subsidence, dam joints, restoration of masonry buildings, and geological stabilizations. Cement production and materials usage continue to rise annually, resulting in more CO₂ emissions and higher energy costs. On the other hand, drinking water production increases in the water treatment plant due to the increasing population, causing, in turn, the production of waste materials, mainly managed to landfill. Consequently, efforts to utilize supplementary cementitious materials to enhance cement compounds' mechanical, economic, and environmental characteristics continue. This study is a unique example of partially replacing cement by calcined drinking water treatment sludge (CDWTS) in the grout production.

The calcination temperature and the fineness were optimised, and the optimum values of 700°C and (25 µm) were ultimately chosen. The chemical and physical properties (Strength activity index (SAI), X-Ray Florence (XRF), specific gravity, and particle size) of the calcined DWTS ash were characterized. CDWTS ash was substituted for 0%, 5%, 10%, and 15% of the cement's weight. Besides, to determine the effect of CDWTS individually on the characteristics of the grout, the amount of water and superplasticizer were kept constant. The experimental work was done in the laboratory to estimate the fresh properties, including (setting time, flow-time, and mini-slump), and hardened properties, including (compressive strength, flexural strength, ultrasonic pulse velocity, and dry density supported with Scanning Electron Microscopy - Energy descriptive X-ray (SEM -EDAX) of the cement grout was produced to investigate its characteristics.

The result showed that the cement grouts with 5% DWTS substituted for cement could be found to have the best overall behaviour and were considered the most promising. Furthermore, it was shown that hardened properties decrease with increasing percentages of replacement (10% and 15%) but stay greater than a reference. According to the fresh state analysis, the workability of cement grout decreased dramatically as the proportion of DWTS increased. This shows that the DWTS can be considered a viable replacement for Portland cement in the grout. The mechanical performance was consistent and supported by the SEM-EDX analysis.

The statistical analysis was also performed utilizing the SPSS program version 26 to predict the hardened properties (compressive strength, flexural strength, and UPV) utilizing Multiple Linear Regression (MLR). For MLR modelling, the mixture proportion and the curing age were input parameters by the standard entry approach. The models' performance was assessed using measures such as the correlation coefficient (R) and coefficient of determination (R^2). The modelling results pointed out that the models used in this study effectively predicted flexural strength and ultrasonic pulse velocity with reasonable accuracy, where the compressive strength has a lower estimation. Based on the outcome of thesis-work, the CDWTS could be considered a viable replacement to cement in grout production, with up to 15% replacement.

Undertaking

I certify that the research work titled “**Characterizing Sustainable Grout for Infrastructure Units**” is my own work. The work has not been presented elsewhere for assessment. Where material has been used from other sources, it has been properly acknowledged / referred.

Signature:

Huda Mohammed Hasan

Date: / 2 / 2023

Dedication

To my comfort and reassurance, to the one who always encouraged me to achieve my ambition: my dear father

To the one who lighted my way to life, To the source of tenderness and tenderness: my beloved mother

To my dearest brothers and sister, who have never left my side and who have always supported me with their prayers and encouraging words

To my wonderful husband, who was very generous in providing me with help morally and financially, and he was a permanent supporter of me through the research.

To the joy that fills my heart and the source of strength for my path, my children.

To my family, friends, and anybody who made a positive difference in my life, even if only by being there or saying something kind, thank you.

I dedicate this humble work to you

Signature:

Huda Mohammed Hasan

Date: / 2 / 2022

Acknowledgements

Thanks be to God, Lord of the worlds, who guides hearts and enlightens insights when He elevates and transcends them and gives me the strength and patience to continue my career.

I am very grateful to my first supervisor, “**Asst. Prof Laith Mohammed Ridha Mahmmod,**” and my second supervisor, “**Asst. Prof Dr. Muhammad Abdulredha,**” for their help, guidance, and continuous efforts during the period of completion of the thesis. Who I was very fortunate to have supervised my research , and I wish them career success. I would also like to thank the honourable **chairman** and **members** of the discussion committee for their valuable comments and additions that enriched the research

Big thanks to our great professor” **Dr. Shakir-Albusultan**” who positively impacted our minds with his help, advice, and scientific giving.

My deepest respect and thanks to my former supervisor “**Dr. Alaa Mohammed Shabban**”, who never hesitated to help me.

I would like to thank the technical staff in both the concrete laboratory and the roads for providing assistance

I would like to thank Miss Ghaida Najim for her assistance during the research period. Also, for my best friends in department of infrastructure.

I would like to thank everyone who helped and supported me, even with a word.

Signature:

Huda Mohammed hasan

Date: / 2 / 2023

Table of Contents

Examination committee certification..	Error! Bookmark not defined.
Supervisor certificate	Error! Bookmark not defined.
Linguistic certificate	Error! Bookmark not defined.
Abstract	v
Undertaking	vii
Dedication	viii
Acknowledgements.....	ix
Table of Contents.....	xi
List of Tables.....	xvi
List of Figures.....	xviii
List of Symbols.....	xxi
Chapter One : Introduction	1
1.1 Introduction.....	2
1.2 Goal.....	4
1.3 Objectives.....	4
1.4 Scope of work	5
1.5 Thesis layout	5
Chapter Two : Literature Review	7
2.1 Introduction	8
2.2 Cement Grout	8
2.3 Supplementary Cementitious Material (SCM)	10
2.3.1 Pozzolanic Reactions.....	10
2.4 Drinking Water Treatment Sludge (CDWTS)	12
2.4.1 Reuse of DWTS	13

2.4.2	Characterization of Calcined DWTS	14
2.4.2.1	Chemical Composition.....	15
2.4.2.2	Physical Properties.....	16
2.4.2.3	The Morphology	17
2.4.3	Calcined DWTS in Cement-Based Material	20
2.5	Summary	25
Chapter Three : Experimental work		27
3.1	Introduction.....	28
3.2	Materials	28
3.2.1	Cement.....	28
3.2.2	Water.....	29
3.2.3	Superplasticizer.....	29
3.2.4	Calcined Drinking Water Treatment Sludge (CDWTS)....	30
3.2.4.1	Preparation of CDWTS	30
3.2.4.2	Strength Activity Method.....	33
3.3	Characterization of CDWTS.....	33
3.3.1	Chemical Properties of CDWTS.....	33
3.3.2	Physical Properties	34
3.3.2.1	Particle Size Distribution	34
3.4	Grout Tests.....	35
3.4.1	Optimization of W/B and Superplasticizer	35
3.4.2	Mixture Proportion.....	36
3.4.3	Fresh Test of Grout	37

3.4.3.1	Setting time.....	37
3.4.3.2	V-Funnel Flow Time.....	38
3.4.3.3	Mini Slump	38
3.4.4	Hardened Test of Grout.....	39
3.4.4.1	Compressive Strength	39
3.4.4.2	Flexural Strength.....	41
3.4.4.3	Ultrasonic Pulse Velocity (UPV)	43
3.4.4.4	Density, Absorption, and Voids in Hardened Grout ..	44
3.4.4.5	Scanning Electron Microstructure and Energy Descriptive X-Ray (SEM).....	46
Chapter Four	Results and Discussion.....	49
4.1	Introduction.....	50
4.2	Optimization of the Temperature of Calcination.....	50
4.3	The Physical and Chemical Properties Of CDWTS	51
4.3.1	The Physical Properties	51
4.4	The Chemical Properties	52
4.5	Optimization of Water /binder Ratio and Superplasticizer	53
4.6	Fresh Properties of Cement Grout	54
4.6.1.1	Setting Time.....	54
4.6.1.2	V-Funnel Flow Time.....	56
4.6.1.3	Mini-Slump.....	56
4.7	Effect of CDWTS on Hardened Propertied of Grout	57
4.7.1	Compressive Strength.....	57
4.7.2	Flexural Strength.....	60
4.7.3	Ultrasonic Pulse Velocity (UPV).....	62

4.7.4	Hardened Density	64
4.8	Microstructural Observation (SEM-EDX)	66
Chapter Five	: Statistical Modelling	75
5.1	Soft Computing Technique and Statistical Modelling	76
5.1.1	General	76
5.1.2	Multiple Linear Regression (MLR)	77
5.1.3	MLR Assumption	78
5.1.3.1	Variables Types	78
5.1.3.2	Sample Size	79
5.1.3.3	Normality of IVs and DV	79
5.1.3.4	Linearity of IVs	80
5.1.3.5	Residuals Homoscedasticity	80
5.1.3.6	Observations Independence	81
5.1.3.7	Absence of Outliers	81
5.1.3.8	Multicollinearity	81
5.1.3.9	Contribution of IVs.	82
5.2	Result of Statistical Analysis	83
5.2.1	Results of the Compressive Strength Production Model ...	83
5.2.2	Results of the Ultrasonic Pulse Velocity Prediction Mode	88
5.2.3	Results of the Flexural Strength Prediction Model	92
Chapter Six	:Conclusions And Recommendations	98
6.1	Conclusions	99
6.2	Recommendations for Further Work	100

List of Tables

Table 2-1: The Chemical Composition of DWTS.	16
Table 3-1: Physical and chemical properties of cement.....	29
Table 3-2: Technical Characteristics of Superplasticizer at 25°C	30
Table 3-3: Physical Properties of CDWTS.....	34
Table 3-4: Mix Proportion of Grout	36
Table 3-5: Classification of UPV (MERMERDAŞ et al., 2020).....	44
Table 3-6: Analysis Condition for SEM.....	47
Table 4-1: mean particle size	52
Table 4-2: Chemical Composition of CDWTS.....	52
Table 4-3: fresh properties of cement paste and grout	54
Table 4-4: Compressive Strength Results of Grout Samples.....	58
Table 4-5: Flexural Strength of Prisms Specimen	60
Table 4-6: UPV Observed with Each Value Is the Average of Three Prisms Specimen.....	62
Table 5-1: Table of Correlation Analysis Among Influencing Factors	84
Table 5-2: Model Summary	84
Table 5-3: Analysis of Variance.....	85
Table 5-4: Regression Coefficients Values.....	85
Table 5-5: Table of Correlation Analysis Among Influencing Factors	88
Table 5-6: Model Summary	88
Table 5-7: Analysis of Variance.....	89
Table 5-8: Regression Coefficients Values.....	90

Table 5-9: Table of Correlation Analysis Among Influencing Factors	93
.....
Table 5-10: Model Summary.....	93
Table 5-11: Analysis of Variance.....	94
Table 5-12:Regression Coefficient Value.....	95

List of Figures

Figure 2-1: initial and final set times for various cement to- water -ratios (Rosquoët et al., 2003).....	9
Figure 2-2: Estimated Quantities of DWTS from Selected Countries (Gomes et al., 2019).....	13
Figure 2-3:Microstructure of Different DWTS (Jia et al., 2021).....	19
Figure 3-1:Calcination Procedure.....	31
Figure 3-2: Sieving A) Sieve No.200.B) Sieve No.500.c) CDWTS ash	32
Figure 3-3: flow chart of a procedure of preparing CDWTS	32
Figure 3-4:XRF-Chemical Composition of CDWTS.....	34
Figure 3-5:Particle Size Distribution apparatus	35
Figure 3-6:Vicat apparatus.....	38
Figure 3-7:a) Flow Time b) Minislump.....	39
Figure 3-8: Cubes and Prisms Specimen.	40
Figure 3-9: Compressive strength device	41
Figure 3-10:Prisms Specimens.....	41
Figure 3-11: Flexural device with the computer system of apparatus	43
Figure 3-12:Oven drying of hardened density of grout specimen	45
Figure 3-13:Apparatus used to determine absorption of hardened grout	46
Figure 3-14: SEM-EDX Apparatus Used in This Study.	47
Figure 4-1: The Effect of Temperature of Calcination on SAI of Cement Past for Both Degree of Fineness, Sieve No.200 And Sieve No. 500.	50
Figure 4-2:particle size distribution.....	52
Figure 4-3: Relationship Between W/b and Compressive Strength....	54

Figure 4-4:Initial and Final Setting Time of Grout with Various Percentages of CDWTS	55
Figure 4-5: The Effect of CDWTS on Flow Time	56
Figure 4-6: The effect of CDWTS on mini slump.	57
Figure 4-7: Behaviour of compressive strength in grouts with CDWTS at different age	58
Figure 4-8: Behaviour of flexural strength in grouts with CDWTS at different ages	61
Figure 4-9: Evolution of the ultrasonic pulse velocity of grouts with the age.	63
Figure 4-10:Effect of CDWTS on absorption of grout sample	65
Figure 4-11:Voids Ratio and Packing Density Versus CDWTS Content.	66
Figure 4-12: SEM observation of cement mixture at 28 days of curing with a) 2 μ m.b)200nm	68
Figure 4-13: SEM observation of GSA5 mixture at 28 days of curing with a) 2 μ m.b)200nm	69
Figure 4-14: SEM Observation of GSA10 Mixture at 28 days of curing with a) 2 μ m.b)200nm	70
Figure 4-15: SEM Observation of GSA15 Mixture at 28 days of curing with a) 2 μ m.b)200nm	71
Figure 4-16: Energy Dispersive Analysis with X-Ray of Grout; (A) Neat Cement; (B) 5% CDWTS (C) 10 % CDWTS; (D) 15 %, Showing the elemental peaks of each material.....	73
Figure 5-1: Probability Curve for Experimental Curve.....	86
Figure 5-2:Linear Probability of Predicted Compressive Strength	87
Figure 5-3: Scatter Plot of compressive strength	88

Figure 5-4: Standardized Residuals Histogram of ultrasonic pulse velocity	91
<i>Figure 5-5: The Standardized Residual Normal P-P of ultrasonic pulse velocity</i>	<i>91</i>
Figure 5-6:Scatter Plot of UPV	92
Figure 5-7: Standardized Residuals Histogram of flexural strength...	96
Figure 5-8: The Standardized Residual Normal P-P of flexural strength	97
Figure 5-9: Scatter Plot of flexural strength	97

List of Symbols

Symbols	Description
C_2S	Belite
C_3S	Alite
Mpa	Megapascal
Na_2SO_4	sodium sulfate
$NaCl$	sodium chloride
PC	Portland cement
W/C	Water-cement ratio
\hat{Y}	the expected outcomes value
E	the random residual error coefficient
B_i	the regression coefficients.
N	the sample size
R^2	the regression coefficient of determination for the U explanatory variable

Abbreviations	Description
$AASA$	activated alum sludge ash
AE	auger electrons
ASR	Alkali silica response
$ASTM$	American standard Testing Materials
AW	Activated Waste
BBB	binary blended binder
BE	Bentonite
BSE	backscattered electrons
CH	calcium hydroxide
CSF	condensed silica fume
$C-S-H$	calcium silicate hydrate
$DWTS$	Drinking water treatment sludge
EDX	Energy descriptive x-ray
FA	Fly ash
$GSA0$	Grout sludge ash zero
$GSA10$	Grout sludge ash10
$GSA15$	Grout sludge ash 15
$GSA5$	Grout sludge ash 5
$HRWR$	High-range water-reducing

<i>LOI</i>	Loss on ignition
<i>MLR</i>	Multiple linear regression
<i>PC</i>	Portland cement
<i>POFA</i>	palm oil fuel ash
<i>SAI</i>	Strength activity index
<i>SCM</i>	Supplementary cementitious material
<i>SE</i>	secondary electrons
<i>SEM</i>	Scanning electron microstructure
<i>SP</i>	Superplasticizer
<i>SPSS</i>	Statistical Package for the Social Sciences
<i>TBB</i>	ternary blended binder
<i>UPV</i>	Ultrasonic pulse velocity
<i>VIF</i>	Variance inflation factor
<i>WTP</i>	water treatment plants
<i>X</i>	x-rays
<i>XRF</i>	x-ray fluorescence

Chapter One : Introduction

1.1 Introduction

One of the products that are economical and suitable for healing structural cracks is grout. A French engineer named Charles Berrigny designed the percussion pump, a grouting technique, 200 years ago and used it to rehabilitate the harbour at Dieppe after it had suffered structural damage. Later, in England, during the construction of the first Thames tunnel at Wapping, Marc Isambard Brunel employed Portland cement as cement grouting materials (Hussin et al., 2007). Then, cement grouting became commonly used during the first decade of the 20th century. Various grout varieties, including cement, cement and sand, clay-cement, slag-cement, resin gypsum-cement, clays asphalt, pulverized fuel ash, and a broad range of colloid and low-viscosity chemical compounds, are utilized nowadays (Hussin et al., 2007).

Grouts made from cement are suspension composites consisting of water, cement, and potentially additives (Celik and Canakci, 2015). Cement grouts' rheological, durability and fresh properties are generally improved by using chemical and mineral admixtures. Adding admixtures to the grout at different compositions changes grout's hardened and rheological properties (Celik and Canakci, 2015). In addition, the production of Portland cement contributes to about 5-7% of anthropogenic greenhouse gases generated, equal to 2.54 billion tons out of the global generation of 36.2 billion tons annually (Celik et al., 2014, Hwang and Huynh, 2015). Thus, the negative effects of cement manufacture have led to increasing the need to find out locally available materials, recycled materials and waste materials which would be suitable alternatives for cement. Another major concern is the growing of population also translates as an increase in water consumption, resulting in more sludge produced by water treatment plants (WTP) (Gastaldini et al., 2015). The amount and composition

of the sludge depend on the volume of water treated in the plant, the process used, and the characteristics of untreated water. It is often the case that water suppliers criticise the quality of untreated water. However, some WTP ends up discharging their waste in water courses, contrary to their interests.

Drinking Water Treatment Sludge (DWTS) is a type of solid waste and must be processed and disposed to prevent environmental damage (Gastaldini et al., 2015).

Last years, worldwide efforts have been made to reuse and/or recycle DWTS to fill the gap between effective drinking water treatment and ecologically sustainable DWTS management (Dassanayake et al., 2015). Thus, it becomes necessary to develop alternative methods for managing DWTS, such as researching the possibilities of utilising it as a building material rather than discarding it in a landfill.

Because of the negative effect associated with conventional Portland cement production economically and environmentally, and the huge quantities of the DWTS produced, which negatively affect the environment. Much research used DWTS in construction materials. Investigations on the application of DWTS in the development of construction and building materials have been carried out (Martínez-García et al., 2012, Hegazy et al., 2012, De Godoy et al., 2020). However, the application of DWTS as Supplementary Cementitious Material (SCM) has great potential that is not been explored enough (Gastaldini et al., 2015, Paris et al., 2016, Mohammed, 2017, De Godoy et al., 2020). This is mainly due to the continuous increasing cost of raw materials and the scarcity of natural resources (Gomes et al., 2019, De Godoy et al., 2019). Since the mineral content of DWTS varies with location, the chemical, physical, and mineralogical characterization must guarantee that the

calcined material becomes able to release reactive silica and alumina, meeting the requirements for application as (SCM) cement-based material.

In conclusion, using DWTS in cement grout has not yet been investigated. Thus, exploring the possibility of using CDWTS as a potential SCM in grout will be examined in this study.

1.2 Goal

The main goal of this research is to investigate the feasibility of using CDWTS as a supplementary cementitious material in a cement-based grout.

1.3 Objectives

To attain the goal above, the following research objectives have been established:

- ❖ Review previous studies about cement-based grout, application, and properties that reflect the quality of cement grout and its pozzolanic reaction. Additionally, characterization of physical and chemical properties of CDWTS, and reuse as SCM.
- ❖ Determine the ideal calcination temperature and degree of fineness for CDWTS based on the optimum strength activity index (SAI).
- ❖ Study the chemical and physical characteristics of the CDWTS.
- ❖ Produce a new grout mixture that contains CDWTS as SCM.
- ❖ Conduct experimental tests to evaluate the performance of the developed grout, including fresh properties (setting times, flow time, and mini-slump) and hardened properties (compressive strength,

flexural strength, ultrasonic pulse velocity, and dry density) supported with Scanning Electron Microscopy- Energy Dispersive X-Ray (SEM-EDX) analysis.

- ❖ Conduct a statistical analysis to support the experimental work and to predict the compressive strength, flexural strength, and UPV based on the mixture proportion and age as input variables.

1.4 Scope of work

The scopes of the work followed in this research could be summarized below:

1. This research investigates the impact of raw materials generated from a local water treatment plant in Karbala / hay-Al-Hussein treatment plant.
2. The XRF of CDWTS was made in the Babylon construction laboratory, while SEM-EDX and particle size were made by the chemical analysis centre for chemical analysis in Baghdad. Indeed, UPV, compressive, and flexural were conducted in the laboratory at the University of Kerbala.

1.5 Thesis layout

The thesis is divided into five chapters whose components are listed below:

Chapter One introduces the background of the research, the problem statement, aim, objectives, the scope of work, and the thesis layout.

Chapter Two reviews cement grout and its properties and CDWTS as SCM in the cement-based product.

Chapter Three describes the materials used in this study (chemical and physical properties), grout preparation, laboratory tests, and methodology followed in this research.

Chapter Four shows laboratory test results about cementitious grout (fresh and hardened properties), spectrum results.

Chapter Five shows the statistical methodology and the results.

Chapter Six shows the conclusions and recommendations for further work.

Chapter Two : Literature Review

2.1 Introduction

Cement Grout has been used in various fields of civil engineering (structural repair, soil, reinforcement foundation, pavement, and tunnel). Cementitious grout is the kind most frequently utilized in infrastructure components that can be enhanced using supplementary cementitious material. One of the by-products recently popularly used as supplementary cementitious material is the drinking water treatment sludge that comes from the water treatment plant. Consequently, this chapter offers a discussion of the previous studies on utilizing the calcined drinking water treatment sludge in cement-composite to pave the way for its use in a cement composite in which the calcined drinking water treatment sludge has not yet been used, which is cement grout.

2.2 Cement Grout

The term "grout" does not explicitly refer to any particular substance (Nicholson, 2014). Depending on the type of binders they incorporate, cement grouts and chemical grouts are the two most common types of grout systems. Epoxy-, polyurethane-, and other polymer-based grouts make up the majority of chemical grouts. Sometimes, a cement-based grout is selected because it is more compatible and environmentally superior. Cement grout has properties (fresh and hardened) that can be enhanced and developed. Many researchers have investigated improving cement grout properties by adding pozzolanic material (Sakib et al., 2020). Grout has several crucial characteristics that must be taken into account. The grout's flowability, bleed, and permeability are all influenced by the water-to-cement ratio, which affects the grout's ability to enter the subsurface (Nicholson, 2014) .

When water separates from the solid grout particles, a layer of water forms on top of the grout, known as grout bleeding (Tan et al., 2005) (Emmelin et al., 2007). The amount of the bleed water in the grout might generate a flow path, affecting the grout's ability to fulfil and close cracks.

Another important property of cement-based grouts is the initial and final setting times. These times can be influenced by the type of cement used, the water content, and the properties of any additives added to the grout mixture (Tan and Zaimoglu, 2004). The initial setting time details the time the grout mixture can no longer be injected, while the final setting time details the point at which the grout mixture begins to harden, and strength develops (Nicholson, 2014). These are important properties to determine as it provides a timescale for when the grout mixture can be used for injection (Tan and Zaimoglu, 2004). Figure 2-1 shows pure (100%) OPC (Ordinary Portland Cement) an OPC CEM I cement's initial and final settings at various water-to-cement ratios. From the figure, it can be concluded that both the initial and final setting times increase with increasing water-to-cement ratio (Rosquoët et al., 2003).

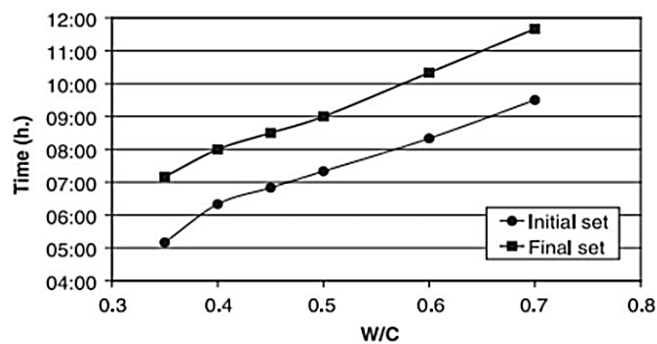


Figure 2-1: initial and final set times for various cement to- water -ratios (Rosquoët et al., 2003).

The mechanical properties of the grout should also be considered if the grouting is for mechanical improvement, hydraulic improvement, or both. Early (2 days) and late (28 days) compressive strength objectives are often used in grouting investigations to guarantee that the grout lasts as long as possible inside the rock mass while maintaining its high strength (Nicholson, 2014).

2.3 Supplementary Cementitious Material (SCM)

A wide range of materials commonly applied in concrete as a supplement to Portland cement is referred to as supplementary cementing materials (SCM)(Thomas, 2013). Defining the nature of the pozzolanic reaction is essential in characterizing the selected SCM.

2.3.1 Pozzolanic Reactions

"A siliceous or siliceous and aluminous substance that chemically combines with calcium hydroxide (lime) to generate compounds possessing cementitious characteristics" is the definition of a pozzolan (Thomas, 2013). Early civilizations employed pozzolans and lime to create hydraulic cement. Nowadays, pozzolans, whether natural or synthetic, are often used in conjunction with Portland cement. Eq 2-1 and Eq 2-2 depict the processes that occur during the hydration of the calcium silicate compounds C_3S (also known as alite) and C_2S (also known as belite) in Portland cement, which results in the copious calcium hydroxide (Thomas, 2013).



Ca(OH), commonly known as portlandite, mostly originates from the hydration of Portland cement, and water mix with pozzolan to generate further cementing product. The pozzolanic reaction is the process that results in a finer pore structure, increasing the durability of mortar and concrete. An explanation of pozzolan's activity in hydraulic cement as (Institute, ACI 232.2R-18) is presented next:

a) The pozzolanic phases of pozzolan react with calcium and alkali hydroxides that are released into solution in the pore structure of the paste by hydrating cement to create more calcium silicate hydrate (C-S-H) gel (cementing matrix)

b) The pozzolanic reaction is enhanced by the heat of hydration, which also accelerates the process.

The calcium silicate gel (C-S-H) that results from the hydration of alite and belite has a variable chemical makeup. The main cementing ingredient of Portland cement concrete, C-S-H, is mostly in charge of giving the concrete strength and other qualities. Alumino ferrite phases (AFm and AFt), which are created by the hydration of the other Portland cement clinker compounds, C₃A and C₄AF, in the presence of gypsum, are found in hydrated Portland cement in addition to C-S-H and calcium hydroxide (CH) (Thomas, 2013).

The product of cement is enhanced when using SCM, such as ground granulated blast furnace slag, silica fume, and fly ash. Nevertheless, their widespread usage is hampered by their restricted availability in some areas and challenges to their worldwide availability, such as the move away from burning coal for power generation (Shamaki et al., 2021). This has interested researchers to engage in discovering fresh SCM.

Wastes or by-product materials have occupied a major element of research projects in terms of modern cement manufacturing due to the wide

range of their chemical properties render them promising in the cement replacement industry (Sun et al., 2015, Van den Heede et al., 2015). There are three advantages of employing industrial waste and by-products in cement-based materials: environmental (abiotic depletion reduction, waste avoidance, energy savings, and decreased CO₂ emissions), economic (using less expensive building materials) and scientific (mortar and concrete's rheological and mechanical properties improvement) (Shamaki et al., 2021). Since sludge from municipal water purification systems may be used as a cementitious material in the grout, it will be the primary focus of this research.

2.4 Drinking Water Treatment Sludge (CDWTS)

Water treatment plants (WTP) are frequently required to treat drinking water in cities. These facilities typically use several procedures, including screening, coagulation, flocculation, sedimentation, decantation, granular filtering, and chemical disinfection (Bonton et al., 2012). Drinking water treatment sludge (DWTS) is the term for wastes or impurities produced in substantial quantities throughout various treatment operations. The increased demand for treated water produced by water treatment plants worldwide has resulted in increasing quantities of sludge by-products generated annually (Horpibulsuk et al., 2016). A typical WTP is thought to generate more than 10,000 tons of sludge every day (Ahmad et al., 2016a). The estimated amount of sludge produced per person across many countries is shown in Figure 2-2.

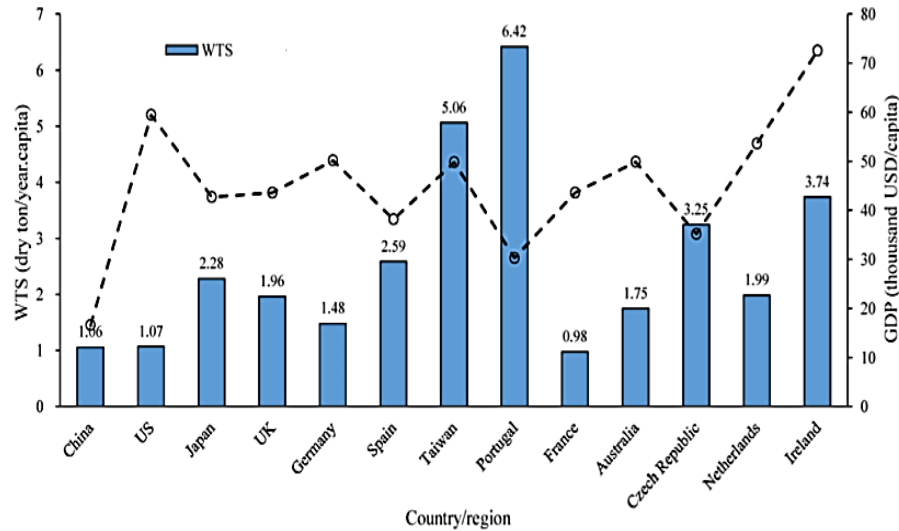


Figure 2-2: Estimated Quantities of DWTS from Selected Countries (Gomes et al., 2019).

Moreover, there are additional problems that local governments and water companies face, such as the danger of water pollution by various contaminants (Belhaj et al., 2016) and the expensive removal of sludge. For instance, in Victoria, Australia, the disposal expense of DWTS topped \$6.4 million annually (Maiden et al., 2015). In the UK, it was £5.5 million (Keeley et al., 2014), and controlling it has become a great concern. Therefore, many investigations have been conducted to reuse the DWTS in various applications.

2.4.1 Reuse of DWTS

Viruses and heavy metals in the DWTS are harmful to the environment. To efficiently reduce the volume of DWTS, oxidize organic matter, immobilize heavy metals, and eradicate pathogens, high-temperature/incineration treatment is used (de Oliveira Andrade et al., 2018). However, this method generates much solid waste. In Brazil, DWTS ash is classified as solid waste and must be treated where it is specified by national

regulation to dispose of in designated areas (de Oliveira Andrade et al., 2018). In China, 29.3% of the DWTS is disposed of in landfills, 26.7% is incinerated, followed by sanitary landfills (20.1%) (Wei et al., 2020).

The most popular approach to dealing with DWTS is landfill disposal. However, landfilling has grown more challenging and expensive because of the increased DWTS output, the shortage of sites, and stiffer environmental regulations (Babatunde and Zhao, 2007). Worldwide, efforts have been made to reuse and/or recycle DWTS in an attempt to fill the gap between effective drinking water treatment and ecologically sustainable DWTS management (Dassanayake et al., 2015). Thus, it becomes necessary to develop alternative methods for managing DWTS, such as researching the possibilities of utilizing it as a building material rather than discarding it in a landfill; especially as SCM in cement composite, therefore, before using must be characterized as having pozzolanic properties

2.4.2 Characterization of Calcined DWTS

The fundamental characteristics controlling the contribution of the SCM especially involve the chemical composition, mineralogical content and the physical characteristics of the substitute materials (Simonsen et al., 2020). In addition to the characteristics of the source water, which are influenced by the bedrock minerals in the catchment area and any contaminants released into the river, the amount of coagulants added during the water treatment process has a significant impact on the physical and chemical properties of DWTS (Shamaki et al., 2021). For recycling and reusing, the characteristics of DWTS from each water treatment plant (WTP) must be characterized even though variations in raw water quality are responsible for changes to treatment

methods and from one treatment plant to another (O'Kelly and Quille, 2010). The important characteristics that must be considered as SCM are chemical and physical properties and the shape of particles that can affect the final product.

2.4.2.1 Chemical Composition

The elemental composition of the pozzolan products is usually performed by the X-ray fluorescence technique (XRF) (Oyedotun, 2018). The XRF technique has many advantages;

- ❖ It is fast.
- ❖ Accurate.
- ❖ Non-destructive.
- ❖ It has a limit of detection in the range of a few parts per million (ppm) of most elements

XRF spectrometry is based on the wavelength-dispersive principle, which states that individual atoms emit a relative abundance of X-ray photons of energy or wavelength feature that can be estimated (Oyedotun, 2018).

The DWTS arrangement of rough dispersed or even colloidal particles is present in the poly-disperse suspension found in the DWTS. Through the application of materials known as coagulants, which are typically responsible for a big proportion of the sludge, the dispersed or colloidal particles available in the raw water are agglomerated and settled down. Aluminium salts ($\text{Al}_2(\text{SO}_4)_3 \cdot 18\text{H}_2\text{O}$), ferric ion salts (e.g., $\text{FeCl}_3 \cdot 6\text{H}_2\text{O}$), and ferrous iron salts (e.g., FeCl_2 , $\text{FeSO}_4 \cdot 7\text{H}_2\text{O}$) are often used coagulants (Sales et al., 2011). Consequently, the DWTS is composed of various concentrations of microorganisms, organic and suspended waste, coagulant products, and

chemical components (Babatunde and Zhao, 2007). The DWTS composition described in earlier studies is shown in Table 2-1.

Table 2-1: The Chemical Composition of DWTS.

<i>Chemical composition</i>	(Andrade et al., 2019)	(Frias et al., 2013)	(Tantawy, 2015)
<i>SiO₂</i>	40.5	41.54	44.21
<i>Al₂O₃</i>	28.5	33.60	16.47
<i>Fe₂O₃</i>	9.5	11.09	4.12
<i>CaO</i>	0.3	0.42	4.62
<i>MgO</i>	0.4	1.51	0.74
<i>K₂O</i>	0.4	3.67	0.31
<i>TiO₂</i>	1.0	1.36	-
<i>SO₃</i>	0.7	0.31	2.02
<i>Na₂O</i>	0.1	-	0.61
<i>MnO</i>	0.1	0.42	-
<i>LOI</i>	18.23	3.31	26.68

The quality of the water sources, the type of coagulants employed, the treatment method involved, and the final quality of the water generated may all affect the percentage of various oxides in the sludge, as shown in Table 2-1. SiO₂ makes up the majority of the sludge in general, followed by Al₂O₃ and Fe₂O₃. Although, CaO, MgO, Na₂O, K₂O, P₂O₅, and TiO₂ are also found in small amounts. The coagulant used (Al or Fe salts) and the concentration of these metals in the raw water is also linked to the amount of Al₂O₃ or Fe₂O₃ in the DWTS.

2.4.2.2 Physical Properties

The strength activity index could be a good indicator of physical properties (Thomas, 2013). A variety of factors that influence the pozzolanic

activity of pozzolans. The most significant variables impacting reactivity are (Thomas, 2013):

- ❖ The type of active phases and how concentrated they are in the pozzolan,
- ❖ The particle sizes
- ❖ Surface area
- ❖ The amount of water used in the mixing process,
- ❖ The temperature

Thermal treatment can affect the pozzolanic reactivity of natural pozzolans (Bondar et al., 2011). This is the reflection of the pozzolan's chemical and mineralogical modifications. Some pozzolans exhibit water loss in glassy or zeolitic phases and in clay minerals when the crystal structure is destroyed. As a result, the pozzolans' pozzolanic activity is increased. The degree and duration of heating may reduce the specific surface area, devitrification, and recrystallization (Thomas, 2013). As a result, the pozzolan's pozzolanic activity is reduced. If the temperature of calcination is elevated while heating pozzolans, combined lime initially rises and then drops. The pozzolan's surface area is lessened throughout the heating process. This implies that there is an ideal thermal treatment for each pozzolan. According to investigations on various natural pozzolans, the ideal temperature was between (700 and 800) °C (Habert et al., 2008).

2.4.2.3 The Morphology

Some pozzolans are microporous, which raises the water needed for the consistency of the cement mixture (Thomas, 2013). Therefore, knowledge of morphology is necessary.

Scanning electron microscopy (SEM) is a high-resolution imaging technique which enables the investigation of the microstructure of an object. Energy dispersive X-ray analysis is used to examine the elemental composition of materials (Jafer, 2017). In the modern SEM imaging process, EDX analysis has usually been used in conjugation with scanning electron microscopy testing to examine the morphology of an object as well as to analyse its elemental composition; in this case, such analysis is called SEM/EDX analysis (Cardell and Guerra, 2016).

A primary electron beam strikes a bulk material and often produces various signals because the electrons are either reflected (scattered) or absorbed. X-rays (X), auger electrons (AE), secondary electrons (SE), backscattered electrons (BSE), and other reactions are generated (Al-Busaltan, 2012). These can allow various modes of observation and/or microanalysis. SEM is the most common observation mode, including capturing secondary and backscattered electrons. On the other hand, Energy descriptive X-ray (EDX) is a microanalytical technique based on the detection of X-rays.

Regarding calcined DWTS, (Jia et al., 2021) examined the morphology of DWTS by SEM. Their study illustrated that DWTS showed irregular particles bonded to the surface of the stratiform layers, the same morphology has been confirmed by (Suksiripattanapong et al., 2015). Figure 2-3 illustrates the SEM of different DWTS wherein (a), Figures 2-4b, and 2-4d show the presence of a regular reticular material that may be the flocculant because it acts as a bridge to bind to colloidal and adjacent particles. Additionally, few crystalline compounds related to the particulate matter in raw water were

shown in Figure 2-4b. For DWTS-3, the SEM reveals the sludge's loose structure and surface fissures. These findings demonstrated the inconsistent morphology of several samples, which may be related to the complicated makeup of DWTS. The morphology depicted in the photos represents just a small percentage of the sludge.

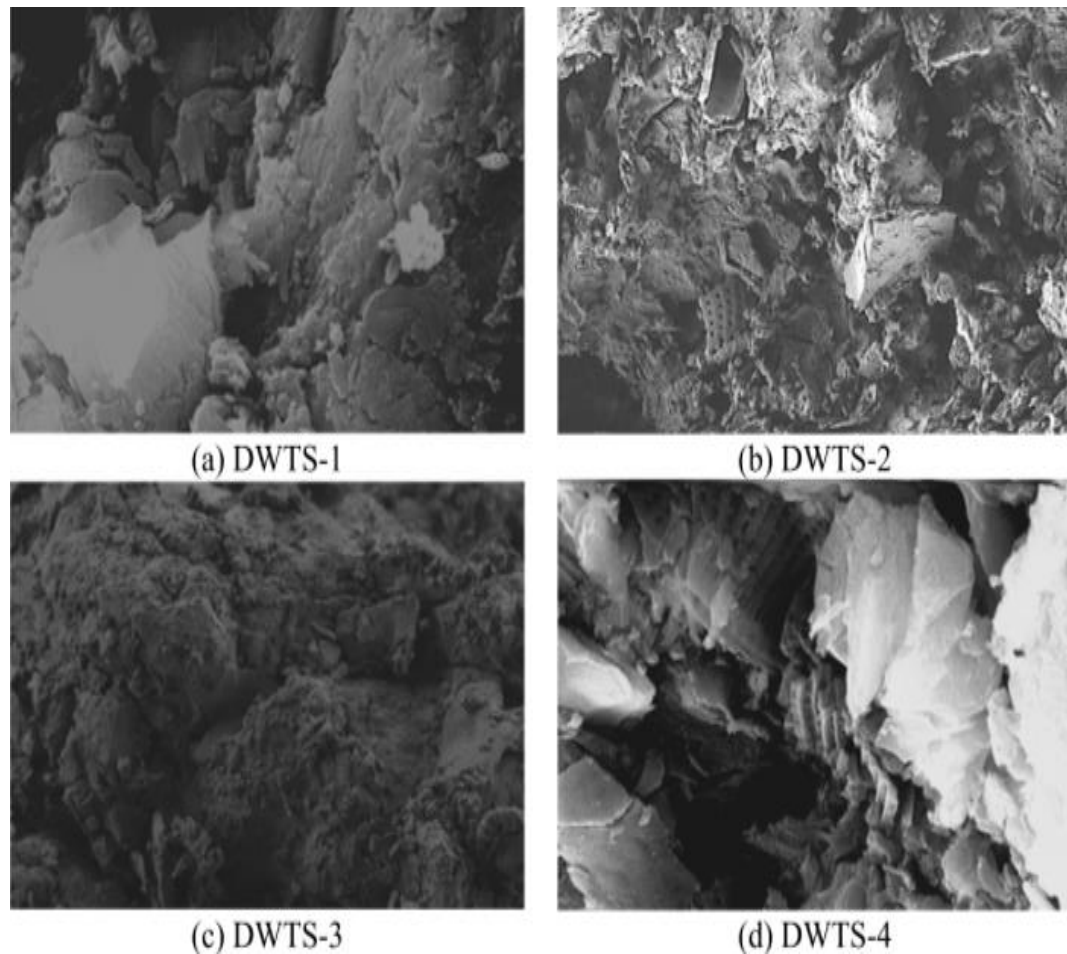


Figure 2-3: Microstructure of Different DWTS (Jia et al., 2021).

Overall, the morphologies of DWTS, including crystals, colloids, and flocculants, contribute to the irregular shapes and rough, porous surfaces of the sludge particles. This is also confirmed by Ahmad et al. (2016b).

2.4.3 Calcined DWTS in Cement-Based Material

The most used cementitious material is Portland cement, whose production and application operations produce 5-8% of the world's CO₂ emissions and 5-6% of the SO₂ emissions together (He et al., 2021). DWTS would benefit from its large-volume usage when partially used to replace Portland cement.

To eliminate microorganisms, immobilize heavy metals, and promote raw DWTS activity, the chemical, physical, and mineralogical characterization of DWTS must ensure that the calcined material can release reactive silica and alumina, trying to meet the criteria for application as SCM, because the mineral composition of DWTS differs depending on location (Gomes et al., 2019).

De Godoy et al. (2020) observed that raw DWTS could have a highly active pozzolanic activity when exposed to high-temperature calcination due to reactive alumina and silica. Some studies have explored the possibility of using calcined DWTS as a SCM in cement-based products. The focus of these experiments was on the pozzolanic activity of calcined DWTS and how it affected the mechanical characteristics of cement.

Frias et al. (2013) conducted extensive research regarding how the activation temperature of inert waste from WTP used as SCM in cement affects the final product. With the aid of various techniques, which include XRF, and SEM, the mineralogy of the reactive products resulting from the pozzolanic activity and the development of the hydrated phases generated during the pozzolanic reaction at 28 days of curing were investigated about the influence of activation temperature. The research has revealed that all the

activated products exhibited significant pozzolanic activity (up to 90 d) at all reaction stages. However, from an economical and energy viewpoint, (600°C) at (2 hr) is the recommended optimal activation condition. Finally, this drinking water waste processing method is appropriate for obtaining future pozzolans standards to produce commercial cement.

In the next year, Frías et al. (2014) analyzed the thermodynamic and pozzolanic characteristics of a Venezuelan DWTS that was activated at 600 °C for two hours and the way it reacts in mixed cement-based materials made with (85%) Ordinary Portland Cement and 15% Activated Waste (AW). The analysis showed that the activated DWTS mainly revealed high pozzolanic properties during the reaction's first 24 hr. The formation of C-S-H gels as the hydration product from the pozzolanic reaction is confirmed by the SEM/EDX and thermodynamic analyses. The binary combination of 15% DWTS and 85% OPC met the physical and mechanical requirements specified in the current European cement standards.

Tantawy (2015) investigated the Microstructure and pozzolanic properties of DWTS calcined for three hours at 600°C–900 °C using X-Ray Diffraction (XRD), SEM, and Thermogravimetric analysis (TGA) techniques and the Chappelle test. The calcination of alum sludge produced a variety of chemical processes, including the production of Al₂O₃ and the crystallization of amorphous silica. In addition, the microstructure and pozzolanic activity of calcined alum sludge is significantly impacted by the calcination process. For calcination increases in temperature up to 800 C°, the amount and density of hydrates formed during hydration declined. However, Alum sludge can be calcined at 800 C° to promote its pozzolanic properties.

(De Godoy et al., 2019) examined the possibility of developing SCM using calcined DWTS. In a WTP in Southern Brazil, sludge samples were

collected in the drying beds and calcined in the laboratory. SEM images have been applied to help with morphological analysis. With Portland cement, physical characterization has been performed through the efficiency of pozzolanic activity, specific surface area, and particle size distribution. Moreover, the results have demonstrated that DWTS is a non-hazardous, non-inert waste that may be used in construction without causing ecological damage. While highly active pozzolan necessitates calcining at 750 °C for 1 hour, sludge samples calcined at 600 °C for 1 hour showed the most promising results when it comes to producing additional cementitious material similar to a normal pozzolan from an energy consumption perspective from a technical, environmental, and economic point of view. Using calcined DWTS as a substitute for additional cementitious material showed excellent technical and environmental potential.

In concrete and as a partial cement replacement, Owaid et al. (2019) made thermally activated alum sludge ash, silica fume, ground granulated blast furnace slag, and palm oil fuel ash are used to create binary and ternary blended binder concrete. After soaking in solutions of 5% sodium sulfate (Na_2SO_4), 5% sodium chloride (NaCl), and 5% water for 90 and 180 days, respectively, the different blended binder concrete's water absorption, porosity, initial surface absorption, sorptivity, and sulfate and chloride resistance were tested. According to the outcomes, the BBB with 15% AASA cement replacement exceeded control, and 20% AASA concretes in terms of durability. Although surface durability was enhanced, inner core durability was not, even with a greater replacement level of 20% AASA. With AASA at

the same replacement levels, all TBB concretes performed better than BBB concretes.

For cement mortar, De Godoy et al. (2020) reported the application of DWTS to develop an SCM. The waste was treated by calcining for an hour at a temperature between 600° C and 800° C. To determine the possible pozzolanic activity of the calcined DWTS and confirm the use as SCM, chemical, mineralogical, physical, and morphological characterization has been carried out. Compressive strength tests have been carried out on cement mortars that use 14%, 35%, and 50% of DWTS in replacement of Portland cement, where DWTS calcined at 600 °C has a high potential for SCM production, as it is proved by chemical and physical analyses in addition to the indicators of pozzolanic activity. The mechanical characteristics of mortars created with 14% and 35% DWTS and calcined at 600°C indicated a possible use in the production of blended and pozzolanic Portland cement.

González et al. (2020) focused on using DWTS ash as SCM, elaborating hydraulic mortars at different calcination temperatures (600 °C and 800 °C) and substitution levels (10 wt% and 30 wt%) of sludge ash for cement. Compressive strength, SEM-EDS, XRF, XRD, and particle size distribution by laser diffraction have all been employed to characterize sludge ash and mortars. 90% of the sludge ash, as indicated by the data, is made up of SiO₂, Al₂O₃, and Fe₂O₃, and it may have pozzolanic activity. There is evidence that the varied ratio of sludge ash to cement considerably impacted the compressive strength of the mortar cubes compared to other factors. According to the study's findings, sludge ash could be regarded as a viable and sustainable choice for the building industry. Although the suggested replacement has advantages, the existence of amorphous SiO₂ necessitates a review of long-term chemical behaviour.

Duan et al. (2020) recycled DWTS as an SCM to prevent the mortar's degradation in response to an Alkali-Silica Reaction (ASR) attack. Before being implemented as a cement replacement, DWTS was grained and calcined at 800 C for two hours. The fine reactive aggregate chosen within that project was glass sand. First, the compressive strength, flexural strength, and water sorptivity of four mortar mix made with 0%, 5%, 10%, and 20% calcined DWTS replacement for cement were assessed. After 28 days of exposure to an ASR-attacked environment, the length of the mortar specimens was monitored for changes, and the uniformity of the mortar was determined using ultrasonic pulse velocity (UPV). Reusing the DWTS proved that 10% replacement greatly enhanced the mechanical properties of mortar. Compared to the reference group, the specimens containing 20% of the calcined DWTS had comparable strength and were more resistant to ASR attack. In addition, a water sorptivity test revealed that mortar with higher calcined DWTS levels may have reduced water capillary absorption.

In the article by Jia et al. (2021), the characteristics of four different types of sludge gathered from various WTP in Australia and China were contrastively compared using XRF, SEM, and XRD. The drinking water sludge ash DWTS, produced by grinding and calcining drinking water treatment sludge, was subjected to an SAI test to quantify its pozzolanic reactivity DWTS. By the study, the major components of DWTS were Al_2O_3 and SiO_2 , and the major crystalline minerals were quartz, kaolinite, and aluminium sulfate hydroxide hydrate, which may be converted into the reactive amorphous state after being calcined at 800 °C. Additionally, the strength activity index (SAI) of the mortar samples produced by DWTS

achieved the requirements, indicating satisfactory pozzolanic reactivity. DWTS might therefore be recycled and used as a pozzolan in cement-based products.

He et al. (2021) discussed the influence of calcined DWTS on the microstructure, specifically in nanoscale microstructure, drying shrinkage and mechanical characteristics of cement-based products were. Meanwhile, SEM and XRD were used to investigate the effect of modified WTS on cement past's microstructure and hydration products. Subsequently, the results proved that the DWTS, as a source of SCM, could be considered a workable and sustainable replacement for cement-based building materials.

2.5 Summary

This chapter reviews the implementation of DWTS in the construction section. It has been shown that many researchers used DWTS in concrete applications. In spite of the novel contributions of previous studies concerning using the calcined DWTS in cement composite, the impact of calcined DWTS on the microstructure of cement-based grout has not been investigated yet. Besides, to the best of the researcher knowledge, no study investigated the application of CDWTS in cement-based grout. Thus, a portion of Portland cement was replaced with CDWTS, and its impact on cement-based grout's hardened and fresh characteristics. The impact of CDWTS on cement pastes' microstructure and hydration products was further studied using SEM-EDX technique.

Chapter Three: Experimental work

3.1 Introduction

The experimental work that has been carried out in this study is described in this chapter. It includes the utilized materials, the testing methodology, and the creation and characterization of novel sustainable grout using CDWTS sludge. Based on the proceeding chapters, the following aspects are highlighted:

- Large quantities of cement are produced annually, which significantly negatively impacts the environment and human health.
- Researchers have employed a variety of alternatives for cement in many building sectors, particularly in the grout.
- One of the materials used as alternatives to cement is DWTS, but this material was not used as a substitute for cement in grout despite its abundance, cheapness, and pozzolanic properties.

Therefore, this chapter details the methods used in this research to investigate the possibility of using CDWTS as a partial replacement for cement in the grout.

3.2 Materials

3.2.1 Cement

According to Iraqi requirement No. 5/2019 Type V with a popular form of Portland cement utilized in this study, was made at the Karbala cement factory. Table 3-1 tabulates the chemical and physical characteristics of cement used in the experimental program .

Table 3-1: Physical and chemical properties of cement

<i>Physical test</i>	<i>Physical Test</i>	<i>limits</i>
<i>Fineness (m²/Kg)</i>	400	≥ 250
<i>Loss Density (gm/cm³)</i>	2.00	Not specified
<i>Initial Setting Time (min)</i>	53	≥ 45
<i>Final Setting Time (hr.)</i>	3.15	≤ 10
<i>Compressive strength at 2 days (Mpa)</i>	17.5	≥ 10 Mpa
<i>Compressive strength @ 28 day (Mpa)</i>	43.7	≥ 42.5 Mpa
<i>Chemical Test</i>	The Result	Limits
<i>SiO₂ (%)</i>	18.8	Not specified
<i>Al₂O₃ (%)</i>	3.9	Not specified
<i>Fe₂O₃ (%)</i>	4.9	Not specified
<i>CaO (%)</i>	62	Not specified
<i>MgO (%)</i>	3.5	≤ 5%
<i>SO₃ (%)</i>	1.3	C ₃ A ≤ 5 % SO ₃ ≤ 2.5 %
		C ₃ A more than 5 % SO ₃ ≤ 2.8 %
<i>Cl (%)</i>	0.02	≤ 1.0
<i>Insoluble Residue (%)</i>	1.0	≤ 1.5
<i>L.O. I (%)</i>	3.4	≤ 4.0 %
<i>Lime Saturation Factor (%)</i>	1.01	-
<i>Al₂O₃/Fe₂O₃ (%)</i>	0.8	-
<i>C₃A (%)</i>	2.0	≤ 3.5
<i>C₃S (%)</i>	72.8	-
<i>C₂S (%)</i>	1.1	-
<i>C₄AF (%)</i>	15.0	-

3.2.2 Water

All grouts used in the present study are prepared with potable water because it is appropriate for cement-based suspension preparation and curing

3.2.3 Superplasticizer

Superplasticizer was supplied by DCP company. It is Hyperplast PC 175, mainly composed of long-chain polycarboxylic polymers. It is Specially designed to significantly increase the effectiveness of the water content in the

mixture. According to the manufacturing company, conforming to American Standards (ASTM C494, 2015), the recommended dosage ranges from 0.4 to 2.5 litres per 100 kg of cement material. Table 3-2 presents the properties of Hyperplast PC 175. The percentage of superplasticizer used to prepare grout mixes optimized depending on trial mixes

Table 3-2: Technical Characteristics of Superplasticizer at 25°C

Colour	yellow Liquid
<i>Water content</i>	1±6.0
<i>specific density</i>	0.02±1.07
<i>chloride content</i>	-

3.2.4 Calcined Drinking Water Treatment Sludge (CDWTS)

3.2.4.1 Preparation of CDWTS

Water treatment sludge was collected from the water treatment plant in Kerbala Project in the Al-Hussein area, which used alum as a coagulant. The plant provides the population with 1000 m³/hr. Samples were dried at 105°C for 24-36 hours to constant mass. Heat treatment was applied at different temperatures (600, 700, 800, and 900 °C) for durations of two hours using a laboratory electric muffle furnace at heating rates of 10 °C/min before cooling to room temperature in ambient air to determine the calcination's optimum range of temperature. Then, grind with a laboratory mill. Also, a similar methodology was previously used by several authors (González et al., 2020, Shamaki et al., 2021, Pham et al., 2021). The appearance of sludge before and after calcination is shown in Figure 3-1. The DWTS is light grey powder, while changed to brownish powder after calcination.

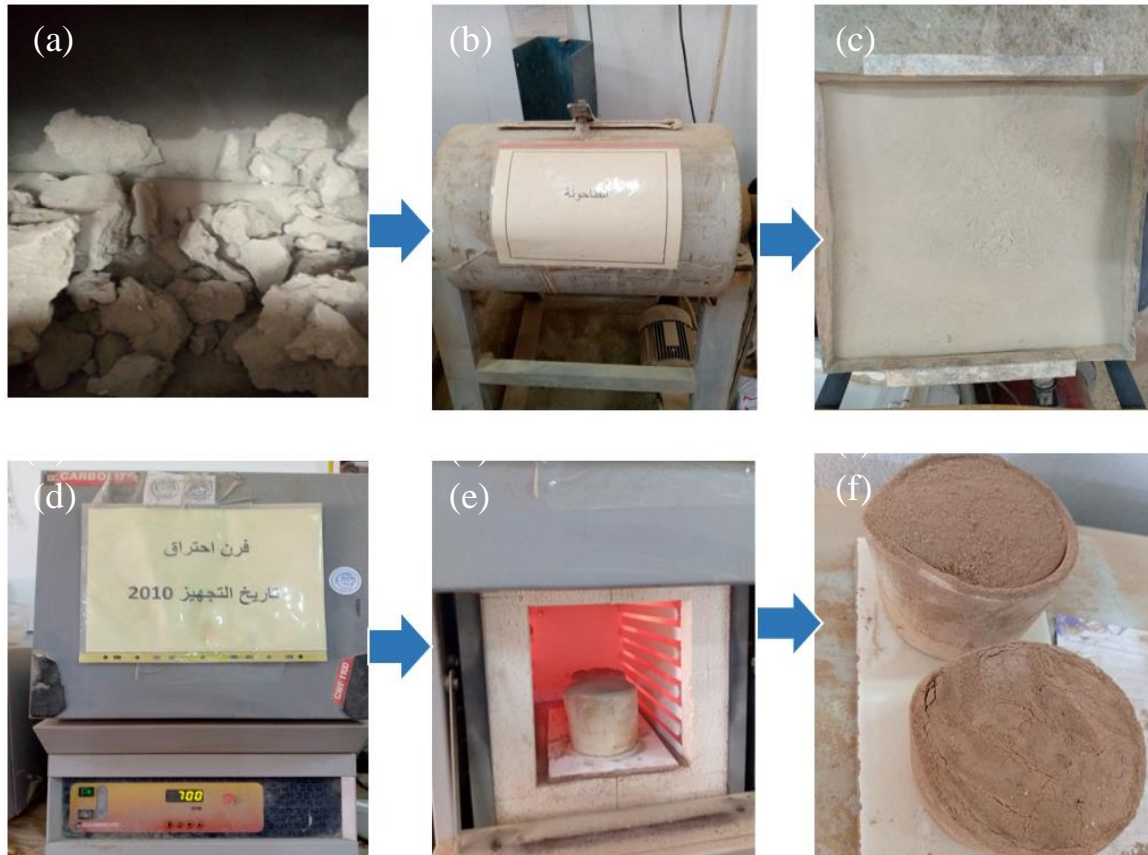


Figure 3-1: Calcination Procedure

After drying, grinding, and calcination, sieving was made with two different size sieves, i.e. ($75\mu\text{m}$ and $25\mu\text{m}$), with the same temperatures to optimize the degree of fineness and the temperature that will depend on the final parameter to process the final product. Figure 3-2 and Figure 3-3 illustrate the sieving procedure and the process of preparation of CDWTS, respectively.

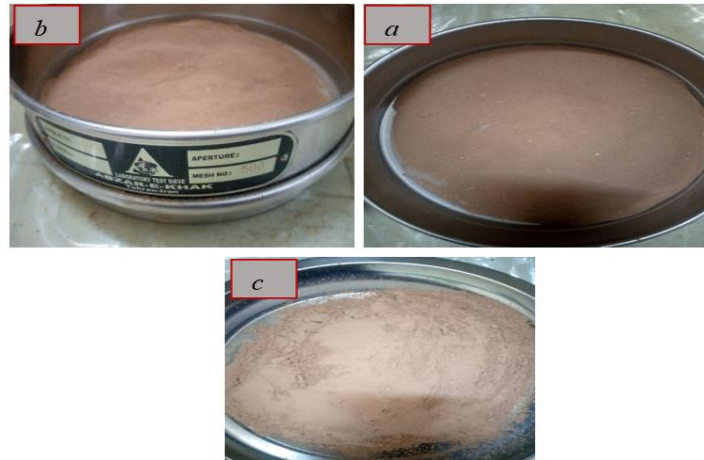


Figure 3-2: Sieving A) Sieve No.200.B) Sieve No.500.c) CDWTS ash

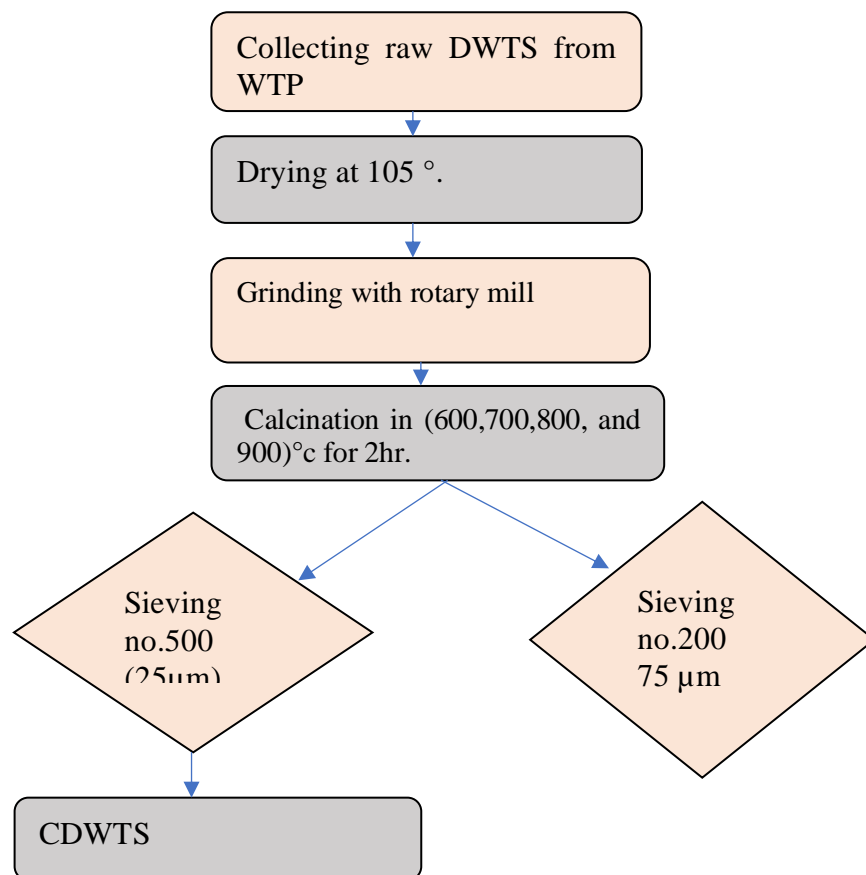


Figure 3-3: flow chart of a procedure of preparing CDWTS

3.2.4.2 Strength Activity Method

Strength activity index (SAI) tests were conducted according to (ASTM, C311M – 17). This is to indicate the pozzolanic activity of the obtained CDWTS and make optimization for choosing the appropriate temperature of calcination as well as the degree of fineness. The cubes were cast and prepared according to (ASTM, C109M – 21) with dimensions of 50 * 50 mm and a replacement percentage of cement of 20%, covered with a plastic sheet and left for 24 hours. The mould was removed and tested for compression to know the SAI. To reduce the consumption of electrical energy sources, the specimen was tested to determine if it maintained the Pozzolanic efficiency indexes, and two degrees of fineness were used (75µm, 25µm).

$$SAI = A/B*100 \quad (\text{Eq 3-1})$$

Where:

A = average compressive strength of test mixture cubes MPa, and

B = average compressive strength of control mix cubes, MPa. According to (ASTM, C311– 22) , the SAI should be at least 75% of the control mix at 7 days and 28 days.

3.3 Characterization of CDWTS

3.3.1 Chemical Properties of CDWTS

The elemental compositions (major oxides and trace elements content) of the CDWTS were analyzed using a Shimadzu EDX-7000 Energy Dispersive X-Ray Fluorescence Spectrometer It was conducted at the Babylon Structural Laboratory shown in Figure 3-4. This high-performance, general-purpose instrument, provides rapid, non-destructive elemental identification and quantification of solid, liquid, and powder samples with no sample preparation required.



Figure 3-4:XRF-Chemical Composition of CDWTS

3.3.2 Physical Properties

The physical properties can be presented by specific gravity conducted by pycnometer apparatus and colour as shown in Table 3-3.

Table 3-3:Physical Properties of CDWTS

Specific gravity	Colour
2.743	Brownish

3.3.2.1 Particle Size Distribution

Analysis of the grain size distribution is crucial to ensuring superior rheological performance, fresh-state characteristics, mechanical properties, and microstructures of cement-based grouts. Dynamic Light Scattering (DLS) measurements is a suitable technique that may allow access to particle size and the presence of agglomerates and aggregates (Linkov et al., 2013). It is a non-invasive, non-destructive, and low-cost technique, and its operation is relatively simple and rapid. With Scattering angle, 9. The PSD is conducted at the chemical analysis center in baghdad.as shown in Figure 3-5 .



Figure 3-5: Particle Size Distribution apparatus

3.4 Grout Tests

3.4.1 Optimization of W/B and Superplasticizer

Underneath the Marsh cone device, which was held up by a platform, there was a measuring jug. The bottom of the Marsh cone was sealed with a finger, after which the mixed grout was poured into the cone all the way to the top. When the cone was filled to the appropriate amount, the bottom end was opened, enabling the grout to flow through the little orifice and into the measuring jar. It was observed how it required to acquire 1750 ml of grout. The collected grout slurry was then moved back into the mixer machine and mixed one more after being given one more dosage of SP. After that, the liquid was once again put into the Marsh cone, and it was timed again to collect 1750 ml of grout. Up till the SP content was ideal, this process was repeated. The point at which adding additional SP would not significantly reduce the length of time required to collect 1750 ml of grout was used to calculate the quantity of SP that would give the grout the maximum fluidity. The same procedure was used for all grout mixtures to determine the appropriate SP concentration for the various w/b ratios and cement with SCM combinations at various

cement replacement levels. In general, it was found that the kind of SCM, cement replacement level, and w/b all had an impact on the initial dose of SP needed to establish the grout's fluidity. The flow of the grout was measured according to (ASTM, C939-16) flow cone. In the flow cone test, 1750 ml of grout is discharged from the cone while the flow's duration is timed. A volume of 1750 ml of water passes through the ASTM cone in 8 seconds.

3.4.2 Mixture Proportion

To examine the effects of CDWTS addition on a grout mixture, water /cementitious material (w/b) needs to be maintained constant because it is a fundamental element that influences both the fresh and the hardened characteristics of a cementitious mixture. Four grout mixtures in total were created. The mixtures had the labels GSA0, GSA5, GSA10, and GSA15 carrying the corresponding percentage (Duan et al., 2020). A 5-l planar-action high-shear mixer was used to prepare all grout mixtures. Before mixing began, the tap water's temperature was the same as room temperature. The water was combined with the optimum superplasticizer dosage for a minute after adding it. The period for mixing started when cement was introduced to the water and superplasticizer mixture. Finally, the grout mixture was thoroughly combined for 7 minutes after the timer started. All grouts exhibited steady temperatures of 24°C when mixing was finished. After the mixing process, the new cement grout's qualities were assessed. The following experiments were performed on newly mixed cement grout, testing the fresh properties and pouring the specimens for hardened properties.

Table 3-4: Mix Proportion of Grout

<i>Mix Label</i>	<i>Material content in the grout (%)</i>			
	<i>Cement (%)</i>	<i>Water (%)</i>	<i>Superplasticizer</i>	<i>CDWTS (%)</i>

<i>GSA0</i>	100	0.45	1.4	0
<i>GSA5</i>	95	0.45	1.4	5
<i>GSA10</i>	90	0.45	1.4	10
<i>GSA15</i>	85	0.45	1.4	15

3.4.3 Fresh Test of Grout

3.4.3.1 Setting time

The Vicat test was conducted in accordance with (ASTM, C191 – 21). These included the initial setting time and the final setting time. Vicat apparatus is shown in Figure 3-6.

Cement setting time depends on factors such as (Senhadji et al., 2012):

- ❖ The fineness of the cement
- ❖ mineral composition of the cement
- ❖ amount of mixing water
- ❖ mineral admixtures
- ❖ additives used
- ❖ and relative humidity



Figure 3-6:Vicat apparatus

3.4.3.2 V-Funnel Flow Time

The Marsh cone test is based on timing how long it takes for a specific volume of grout to flow through a flow cone. According to (ASTM, C939-16). This investigation uses a metal cone with a capacity of 1725 ml and an outlet-pipe diameter of 12.7mm. Figure 3-7 (a) shows the apparatus to assess the flow duration. The funnel is moist before each test. With the outlet sealed, 1800 ml of the grout is poured into the cone. The bottom end of the Marsh cone is then sealed with a finger, and the mixed grout is poured into the cone to the top. Once the cone has been filled to the necessary level, the cone's bottom end is opened, allowing the grout to pour. The flow time is calculated for groups with and without CDWTS, and replacement percentages of 0%, 5%, 10%, and 15. All measurements are conducted at an ambient temperature of $20 \pm 8^{\circ}\text{C}$. The flow time of 1725 ml of water through the ASTM cone is 8 s

3.4.3.3 Mini Slump

Fresh grout's spreading or diffusion ability can be characterized by its mini slumps. A small amount of grout is discharged from a small funnel and

allowed to flow against its weight. This is a type of free-flow test method. The finished diameter provides information about material flow (Ganaw, 2013). According to (ASTM, C143M – 20), mini-slumps testing is shown in Figure 3-7 (b).



Figure 3-7:a) Flow Time b) Minislump

3.4.4 Hardened Test of Grout

3.4.4.1 Compressive Strength

To check the quality of cementitious materials, compressive strength is a criterion that is frequently utilized. The compressive strength tests for the grout cubes mixed and cast at room temperature 20°C were performed according to (ASTM, C942 – 10) for ages 1, 3, 7, 14, 20, and 28 days. Table 3-4 shows the percentage of CDWTS added to the cement paste during casting, which range from 0% to 5%, 10%, and 15% by weight of cement. For

each combination, 18 cubic mould specimens were cast, as indicated in Figure 3-8. The grout specimens were then dried for 24 hours at 20°C and 95% relative humidity. The universal testing machine crushed the specimens wearing face up (Figure 3-9) after demoulding up to failure. The load was applied without shock. For each combination, three cubic specimens were evaluated. compressive strength was determined according to Equation 3-2.

$$f_c = \frac{F}{A} \quad \text{Eq 3-2}$$

Where:

f_c is the compressive strength, in Megapascals (MPa);

F is the maximum load at fracture, in Newtons (N);

A is the area of the platens in square millimetres (mm²).



Figure 3-8: Cubes and Prisms Specimen.



Figure 3-9: Compressive strength device

3.4.4.2 Flexural Strength

Flexural strength can be a good indicator of how brittle-hardened cement-based grouts are. The flexural strengths tests were conducted with prisms (Figure 3-10) (ASTM, C348 – 19). Specimens were poured with the mixture, let to harden, then remoulded and cured in water, with curing times ranging from one to twenty-eight days. On the day of the test. The samples were removed from the curing pools and tested for flexural strength device.



Figure 3-10: Prisms Specimens

using a flexural equipment having a test rig for 3-point loading arrangement as shown in Figure 3-11. The prism sample was placed symmetrically on supports A and B projecting 30mm from both ends, while load was applied centrally at point F. The load at failure was used to compute the flexural strength of the sample in line with Equation 3-2. The average of three prisms was taken as the flexural strength.

$$f_s = \frac{1.5 \times F \times l}{b^3} \quad \text{Eq 3-3}$$

Where:

f_s = flexural strength, in mega pascals;

b = side of the square section of the prism, in millimetres;

F = load applied to the middle of the prism at fracture, in Newtons;

l = distance between the supports A and B, in millimetres.

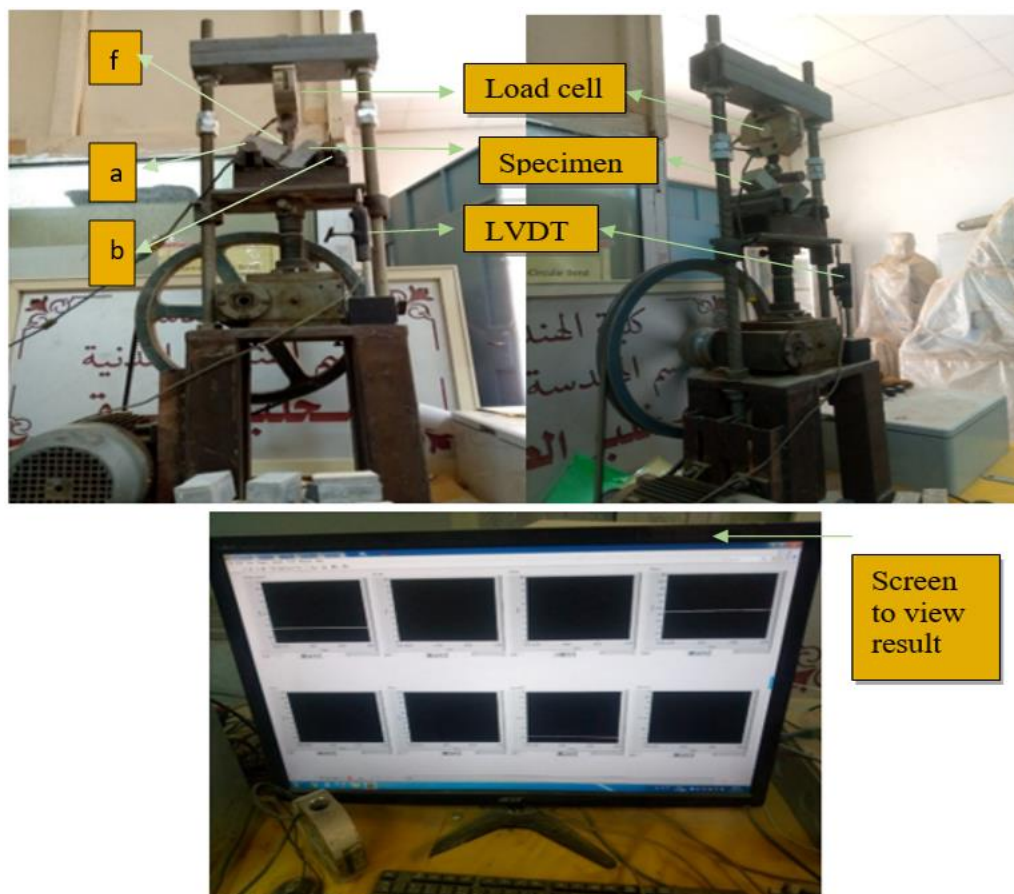


Figure 3-11: Flexural device with the computer system of apparatus

3.4.4.3 Ultrasonic Pulse Velocity (UPV)

UPV is a non-destructive test used to evaluate the quality and compressive strength of concrete and other solid building materials. It uses an ultrasonic pulse to offer information on the regularity of concrete, cavities, fractures, and faults. A Pundit-lab apparatus measuring in a wide range of intervals from 24 to 500 kHz was used for the UPV testing with gel to ensure that the acoustic signal can be well-received. The longitudinal pulse wave velocity of the prisms specimens is determined by the longitudinal vibration pulses applied in contact with the specimen surface (ASTM, C597 – 16). After travelling through the specimen, the pulses are electronically received in pulse velocity measurements to understand the material homogeneity.

Previous research showed that several quality classes might be used to determine how challenging the sample is. The magnitude of measurements can be interpreted by some categorizations given in Table 3-5

Table 3-5: Classification of UPV (MERMERDAŞ et al., 2020)

<i>Class</i>	UPV (m/s)	Definition
<i>1</i>	< 2500	Very low velocity
<i>2</i>	2500-3500	Low velocity
<i>3</i>	3500-4000	Middle velocity
<i>4</i>	4000-5000	High velocity
<i>5</i>	> 5000	Very high velocity

3.4.4.4 Density, Absorption, and Voids in Hardened Grout

The durability of hardened cementitious materials is significantly influenced by water absorption. Reduced water absorption can significantly increase cementitious materials' longevity and long-term performance under challenging situations. Grout's bulk density, absorption after immersion, apparent density, and volume of permeable pore space (voids) ratio were all calculated using the formulae provided in the standard (ASTM, C642-21), and the test method helped to collect the data required to convert grout's mass and volume. After 28 days of curing, the specimen is removed from water and subjected to the dry density method as follows:

- i. Drying the grout specimen in the oven for 24 hr (Figure 3-12) and then waiting until the difference between two successive readings was less than 0.05 %, the final weight recorded as A.



Figure 3-12:Oven drying of hardened density of grout specimen

- ii. Put the specimen in the water tank for not less than 48 hr. until the difference between the readings becomes more than 0.05%, then let them out and dry the surface of the specimen and weighted as B.
- iii. boiling the specimen for a duration not less than five hr., then cooled to atmosphere temperature, let them out of water, dry the surfaces, and record the weight as C.
- iv. Suspend the specimen (Figure 3-13), after immersion and boiling, by a wire and determine the apparent mass in the water. Designate this apparent mass as D.

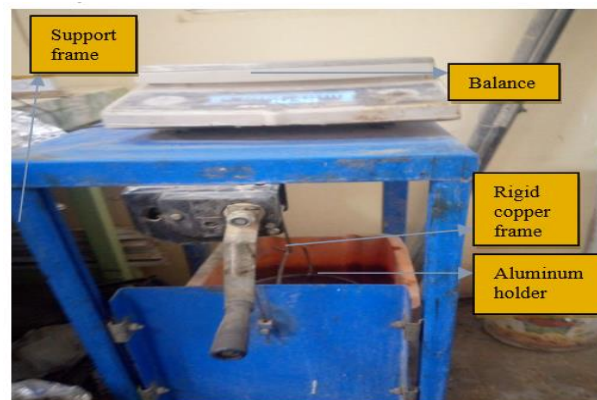


Figure 3-13: Apparatus used to determine absorption of hardened grout

$$\text{Absorption after immersion, \%} = [(B - A)/A] \times 100 \quad (\text{Eq 3-4}).$$

$$\text{Absorption after immersion and boiling, \%} = [(C - A)/A] \times 100 \quad (\text{Eq 3-5})$$

$$\text{Bulk density, dry} = \left[\frac{A}{C-D} \right] \cdot \rho = g1 \quad (\text{Eq 3-6})$$

$$\text{Bulk density after immersion} = [B/(C - D)] \cdot \rho \quad (\text{Eq 3-7})$$

$$\text{Bulk density after immersion and boiling} = [C/(C - D)] \cdot \rho \quad (\text{Eq 3-8})$$

$$\text{Apparent density} = [A/(A - D)] \cdot \rho = g2 \quad (\text{Eq 3-9}).$$

$$\text{The volume of permeable pore space voids, \%} = (g2 - g1)/g2 * 100 \quad (\text{Eq 3-10}).$$

Where:

A = mass of oven-dried sample in air, g

B = mass of surface-dry sample in the air after immersion, g

C = mass of surface-dry sample in the air after immersion and boiling, g

D = apparent mass of sample in water after immersion and boiling, g

g1 = bulk density, dry, g/cm³ and

g2 = apparent density, g/cm³

ρ = density of water = 1 Mg/m³ = 1 g/cm³

3.4.4.5 Scanning Electron Microstructure and Energy Descriptive X-Ray (SEM)

SEM-EDX is one of the most adaptable methods for analyzing cementitious materials. It is frequently used on flat, polished samples in backscattered mode. The SEM-EDX model (TSCAN-MIRA3) instrument shown in Figure 3-14 is used in this study with accelerating voltage of 15, as illustrated in Table 3-6. It has been established that porous materials'

macroscopic characteristics, such as strength, impermeability, and deformation, are significantly influenced by their pore structure. The performance of the slurry can only be enhanced by looking at the hardened paste's microstructure qualities and evaluating how they relate to macroscopic attributes. Since pastes prepared from mixing of different cementitious materials) tend to be non-conductive, the samples for these analyses were coated with a thin layer of an electrically conductive material. Gold was used as a coating material in this study, and the test was made at period of 28 days of curing.

Table 3-6: Analysis Condition for SEM

Accelerating Voltage (kV):	15.0
Beam Current (pA):	750.0
Magnification:	5000
Live Time (s):	5
Preset Time (s)	5



Figure 3-14: SEM-EDX Apparatus Used in This Study.

Chapter Four Results and Discussion

4.1 Introduction

The observations of the various tests conducted, such as optimization the temperature of calcination and the characteristics the chemical and physical properties of CDWTS (XRF and particle size distribution) then tested within (fresh and hardened properties of cement grout), and SEM-EDX analysis have been analysed. The results of the analysis are discussed in the subsequent sections. Lab test results and detailed analysis are presented in this chapter. The findings show the qualities of the finished cementitious grout.

4.2 Optimization of the Temperature of Calcination

To optimize the temperature of calcination, various temperatures were used to know the potential pozzolanic of CDWTS by SAI at two degrees of fineness were used: sieve No.200, and sieve No.500, The result of SAI of at different temperature is illustrated in Figure 4-1

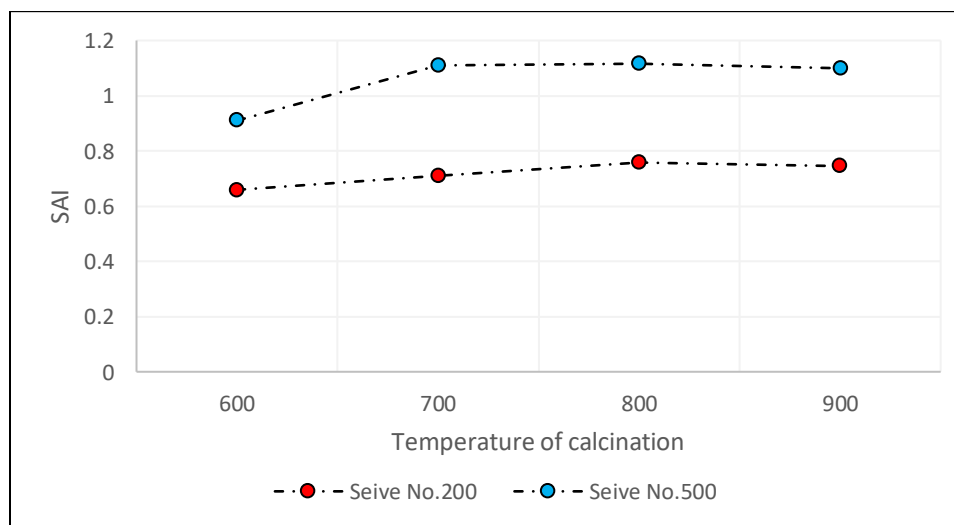


Figure 4-1: The Effect of Temperature of Calcination on SAI of Cement Past for Both Degree of Fineness, Sieve No.200 And Sieve No. 500.

As shown in the previous figure, the result of SAI reveals that SAI increased with temperature of calcination that increased due to the loss of organic material with the temperature of calcination and then decreased (de Azevedo Basto et al., 2019) . For sieve No.200 the increase in SAI of CDATS was lightly remarkable with the temperature increasing. For sieve No .500 the SAI increased over the SAI of sieve No.200. However, the increase was dropped slightly after the temperature (800) °c.

The increase in SAI was due to reactive silica and alumina Subsequently, enhancement in pozzolanic properties ,and the reduction take place after that was related to the existence of an ideal thermal treatment for each pozzolan (de Azevedo Basto et al., 2019). According to investigations on various natural pozzolans, the ideal temperature is between (700 and 800) °C (Thomas, 2013) . On other hand, from a view of conservation of energy a temperature of (700)°c was adopted as the final degree and fixed to prepare CDWTS .

4.3 The Physical and Chemical Properties Of CDWTS

4.3.1 The Physical Properties

The physical properties of CDWTS including grain size distribution has a major influence on cement properties such as water demand, setting and hydration reactions which eventually control the strength development of final composite(Simonsen et al., 2020). The grain size- distribution can have a major influence on the reactivity of the SCM. A well-graded particle size distribution enforces packing density and optimizes pore structure while a high fraction of finer particles can enforce reactivity. However, it can decrease workability due to an excessive water demand.

The mean particle size is 420nm as illustrated in table 4-1.

Table 4-1:mean particle size

Peak No.	S.P.Area Ratio	Mean	S. D.	Mode
1	1.00	420.6 nm	17.4 nm	423.3 nm
2	---	--- nm	--- nm	--- nm
3	---	--- nm	--- nm	--- nm
Total	1.00	420.6 nm	17.4 nm	423.3 nm

Cumulant Operations

Z-Average : 3127.3 nm
 PI : 1.566

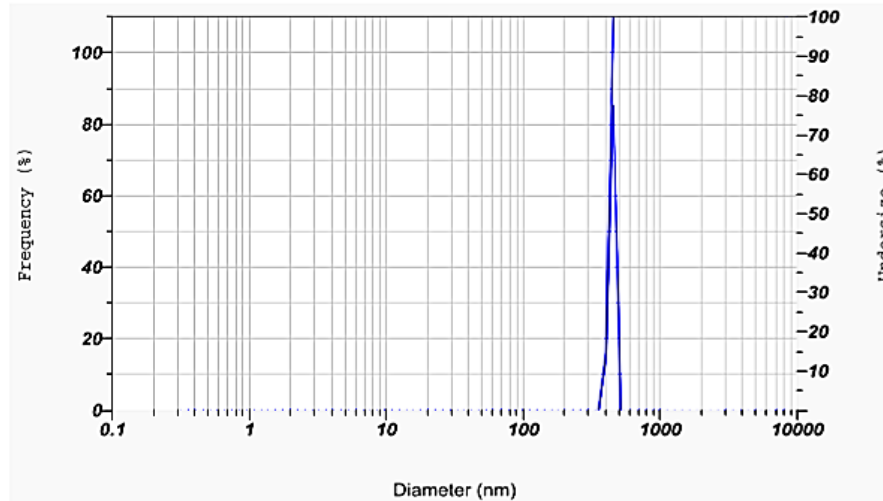


Figure 4-2:particle size distribution

The sharply defined PSD peaks in the studied sample as shown in Figure 4-2 point to a relatively monosized (in relation to the size spectrum) particle arrangement.

4.4 The Chemical Properties

The chemical analysis of CDWTS is achieved through using XRF technique that is used to detect the major oxides contribute of pozzolanic material as presented in Table 4-2.

Table 4-2:Chemical Composition of CDWTS

Chemical properties of CDWTS						
<i>Composition</i>	SiO ₂	Al ₂ O ₃	Fe ₂ O ₃	CaO	MgO	SO ₃
<i>Percentage (%)</i>	38.04	10.96	10.14	16.24	3.65	2.87

Depending on XRF analysis which used to determine the chemical components of CDWTS (see Table 4-2), the findings revealed that SiO_2 and CaO made up the majority of the CDWTS. Al_2O_3 and Fe_2O_3 come second and third respectively. Other oxides, such as SO_3 , and MgO , were also observed to be close to those found in other investigations (Yagüe et al., 2005, Ramirez et al., 2018). The coagulant used in the water treatment process immediately reflected the chemical makeup of the sludge. This may have been connected to the presence of Al_2O_3 . MgO , which is an expansive component can cause volume instability by delayed expansion (Snellings, 2016). The MgO content should thus not exceed 4.0% (Simonsen et al., 2020). These findings suggest that the chemical properties of various DWTP sludges can be related to regional geological features (such as watershed adduction) and the coagulant utilised in the WTP's water treatment procedure. Finally, according to ASTM C618-22 and depending on the chemical composition, the material can be considered as SCM.

4.5 Optimization of Water /binder Ratio and Superplasticizer

To optimize the superplasticizer and W/b ratio, start with the moderate percent within the range dosage and optimize the water /cement ratio flow time by recording the flow time in each trial to choose the optimum w/b ratio.

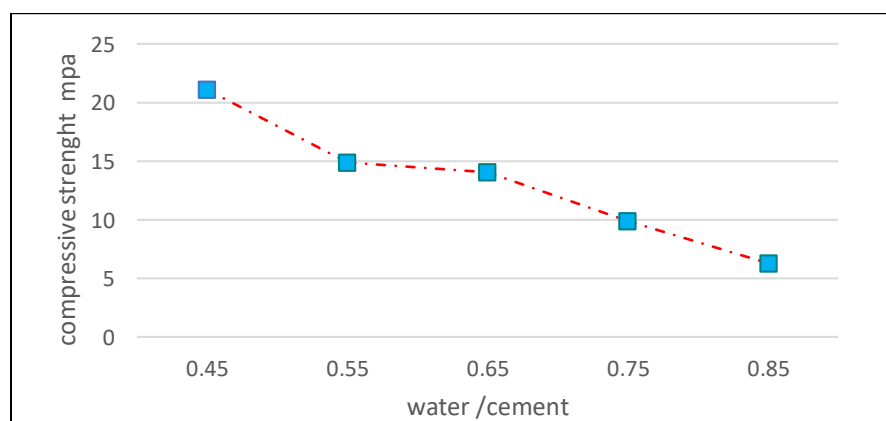


Figure 4-3: Relationship Between W/b and Compressive Strength

Figure 4-3 show the relationship between the water with compressive strength. All mixtures benefited from a higher SP dose, which improved their workability and flowability while diminishing their cohesiveness. The larger dose of SP shows that a greater volume of water results in a shorter flow rate, indicates that. Since the grout used in different infrastructure units needs to be somewhat fluid, and the compressive strength decreases as the water percentage increases, a water ratio of 0.45 were optimal. A significant component determining the rheological qualities of grout is the grout mixing process. The number and size of cement particle agglomerates decrease with improved mixing, increasing the fluidity of the grout (Williams et al., 1999).

4.6 Fresh Properties of Cement Grout

4.6.1.1 Setting Time

Setting time was measured to determine the effect of the replacement of CDWTS on the workability of grout, as tabulated in Table 4-3 and Figure 4-4.

Table 4-3: fresh properties of cement paste and grout

Cement paste	Cement	CDWTS5	CDWTS10	CDWTS15
<i>Initial setting time (min)</i>	123	131	151	174
<i>Final setting time (min)</i>	393	336	358	368
Cement grout	Mixture label			
Properties	GSA0	GSA5	GSA10	GSA15
<i>Initial Flow time(sec)</i>	16.51	18.13	19.26	19.56
<i>Final flow time(sec)</i>	28.24	33.53	36.56	32.27
<i>Flow spread (cm)</i>	30.2	29.75	29.67	29.62

The experimental results in Table 4-3 illustrate how the CDWTS content increases setting times. All the recorded initial setting times exceeded 45 minutes, and all the recorded final setting durations were less than 420 minutes, which correspond to the minimal and maximal intervals, respectively, that are required by (ASTM, C191 – 21)

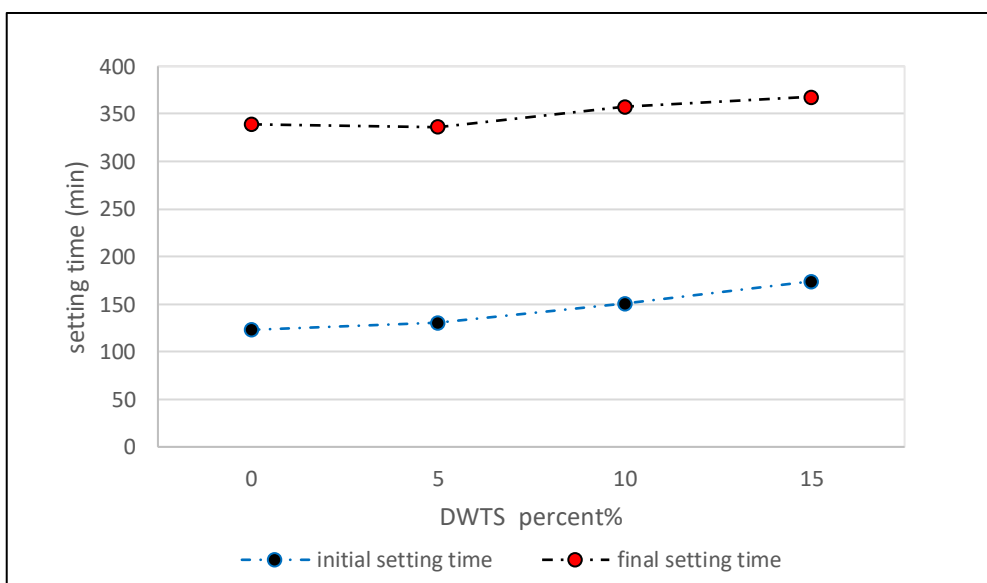


Figure 4-4: Initial and Final Setting Time of Grout with Various Percentages of CDWTS

From the results obtained, it can be observed that the increase of the quantity or percentage of the CDWTS incorporated in the cement grout has a considerable effect. It should also be noted in Figure 4-4 that the progressive addition of the pozzolan influences the setting times. It is seen that setting times (initial and final) increase proportionally with the increase in the quantity of CDWTS. This is likely because the binder's hydration rate slows down with increasing pozzolanic addition. Yetgin and Çavdar (2006) linked

the decreased heat of hydration evolution to the later setting times (Yetgin and Cavdar, 2006).

4.6.1.2 V-Funnel Flow Time

The grout mixtures' deformability and fluidity (workability properties) are tabulated in Table 4-3 in the sixth and seventh row.

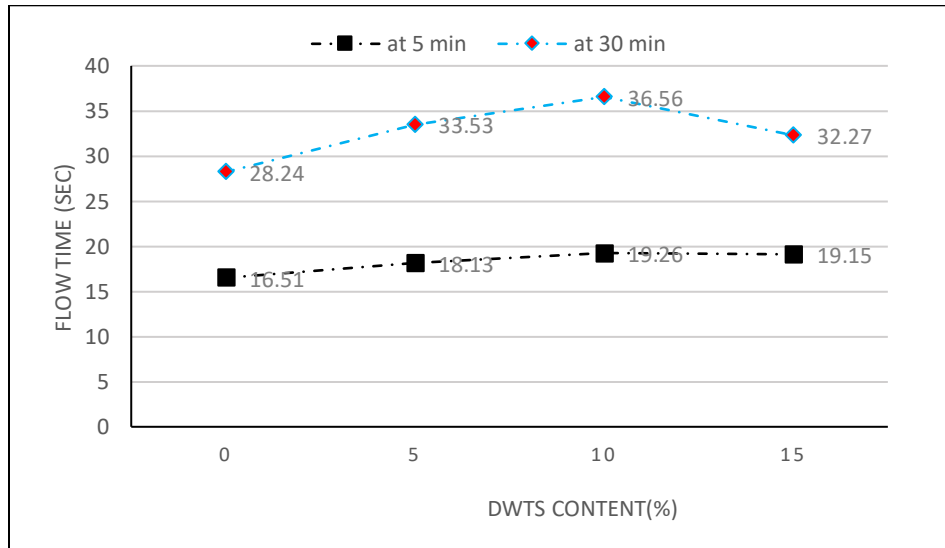


Figure 4-5: The Effect of CDWTS on Flow Time

In addition, as shown in Figure 4-5, increasing the CDWTS amount in the grout mixtures decreases the flow time at $w/b = 0.45$. When using a larger quantity of CDWTS in the grout mixes, the flow duration of the marsh cone lengthens as a sequence reduction in the flowability and deformability. The reason of the reduction in the flowability and deformability of grout mixtures when cement is replaced with CDWTS is attributed to the higher water absorption capacity of CDWTS.

4.6.1.3 Mini-Slump

The grout mixtures' deformability and fluidity (workability properties) are listed in Table 4-3, and plotted against CDWTS as shown in Figure 4-6.

According to this figure, an increase in the CDWTS amount in the grout mixtures decreases the diameter of the mini-slump flow due to irregular particles bonded to the surface of the stratiform layers, which confirmed by (Suksiripattanapong et al., 2015).

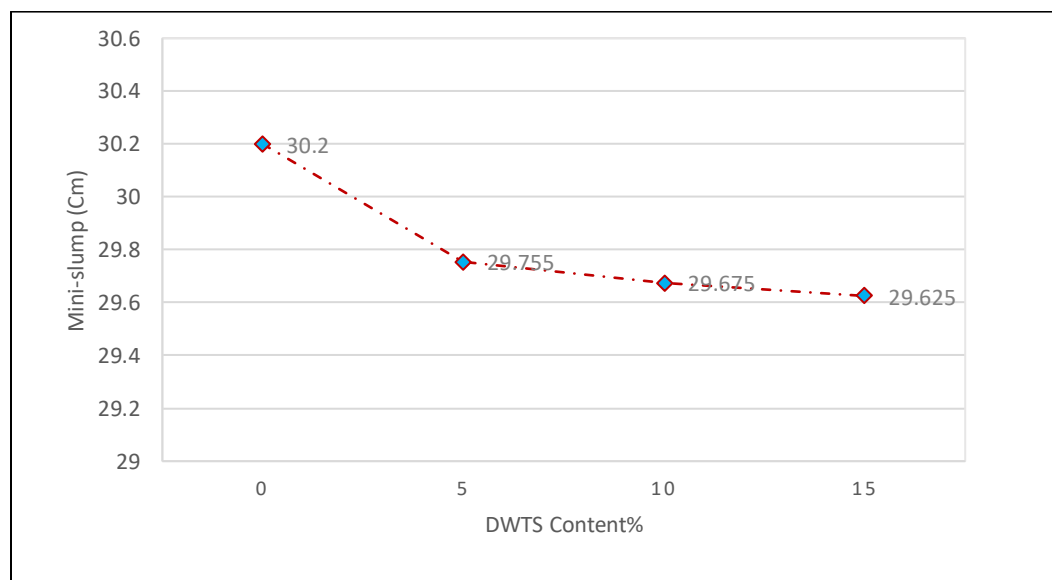


Figure 4-6: The effect of CDWTS on mini slump.

Moreover, adding more CDWTS to grout mixes clearly decreased their workability. The greater water absorption capacity of CDWTS is responsible for the decrease in the workability of grout samples while using CDWTS. There is also the fact that an increase in plasticity and cohesiveness brought on by the paste volume makes grout mixes less fluid (Şahmaran et al., 2006, Yahia et al., 2005).

4.7 Effect of CDWTS on Hardened Properties of Grout

4.7.1 Compressive Strength

One of hardened cement paste's most important mechanical properties is its compressive strength. Hence, it is assessed at ages 1, 3, 7, 14, 20, and

28-days using CDWTS. The compressive strengths of all cement paste samples are tabulated in Table 4-4.

Table 4-4: Compressive Strength Results of Grout Samples

Compressive strength at various ages (Mpa)						
Mix. Lab	(1) day	(3) days	(7) days	(14) days	(20) days	(28) days
GSA0	4.6	15.1	17.3	23.6	23.7	25.9
GSA5	14.0	26.8	27.7	31.0	37.3	39.3
GSA10	11.0	22.3	22.8	27.3	34.6	36.4
GSA15	8.5	17.6	20.5	25.8	29.4	29.5

*Each value actors as the average of three cubic

In addition, the compressive strength of various mixture against the curing age are plotted in Figure 4-7.

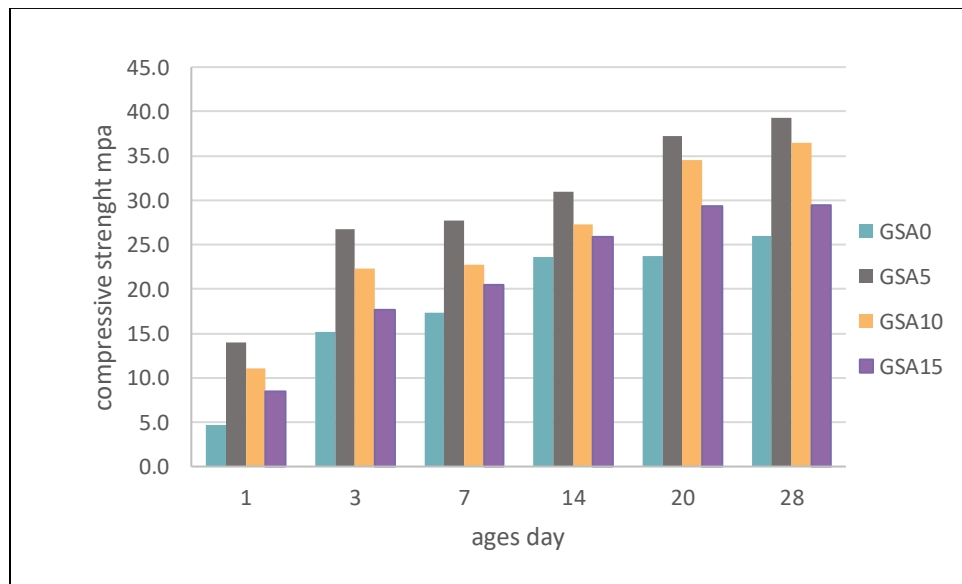


Figure 4-7: Behaviour of compressive strength in grouts with CDWTS at different age

The figure above shows the behaviour of compressive strength of grout mixtures across the ages of 1, 3, 7, 14, 20 and 28 days of curing various percentages of cement replacement with CDWTS. It can be noticed that the

trend of compressive strength increased with the age of all mixtures. Also, the rate of development of compressive strength at an early age was higher than the rate of development in the property in the late stage. On the other hand, the overall behaviour of the mixture shows considerable improvement in compressive strength with GSA5, GSA10, and GSA15 with respect to the reference mixture (GSA0). The mixture with 5% replacement revealed the optimum enhancement in the property. However, the GSA10 and GSA15 were lower than the GSA5 but higher than the control mixture. Therefore, it is possible to produce grout with the preceding percentage of CDWTS from the point of strength and economy. Compressive strength development for the early ages was higher than that in the late ages. For the age of 1 day, the compressive strength development for GSA5, GSA10 and GSA15 was 201%, 137%, and 39%, respectively, compared to the reference mixture. For three days, the compressive strengths were 76%, 47% and 16%, respectively, compared to the reference mixture. For seven days, the compressive strengths were 59 %, 31%, and 18 %, respectively, with respect to the reference mixture.

For 14 days of curing, the rate of increase for the mixture GSA5, GSA10 and GSA15 were 30%, 15%, and 9%, respectively, with respect to the reference mixture. For 20 days of curing, compressive strengths were 58 %, 45% and 11%, respectively. For 28 days of curing, compressive strengths were 51 %, 38%, and 12%, respectively, with respect to the control mixture. In other words, the rate of compressive strength development increases rapidly in the early stage quicker than in the latest age. The replacement of CDWTS caused an increase in compressive strength is associated with a decrease in the apparent porosity (Laidani et al., 2022). The result was confirmed by De Godoy et al. (2020)

The pozzolanic activity from CDWTS could explain the compressive strength improvement. The CDWTS reacted with CH, generated through the cement hydration and formed extra in the binder matrix, improving the grout's mechanical performance (Papadakis, 1999). Less cement also led to a lower amount of CH, which could slow down the formation of the C-S-H generated via pozzolanic reaction in the secondary hydration (Duan et al., 2020). This behaviour could have occurred because of the finer particles' higher pore-filling capacity due to the effective utilization of dry mixing, which raised the content of cement-based materials' compressive strength. Combined effectiveness of filler effect and pozzolanic capability resulted in high compactness through mechanical particle filling and further formation of calcium-silicate-hydrate (C-S-H) gels. This result were previously confirmed by He et al. (2021) and De Godoy et al. (2020).

4.7.2 Flexural Strength

The flexural strength is often relied upon an indicator of structural performance for brittle dental materials. The flexural strengths of the grouts for samples GSA0, GSA5, GSA10 and GSA15 are listed in Table 4-5 and Figure 4-8.

Table 4-5: Flexural strength of prisms specimen

flexural strength at various ages (Mpa)						
Mix. Lab	<i>(1) day</i>	<i>(3) days</i>	<i>(7) days</i>	<i>(14) days</i>	<i>(20) days</i>	<i>(28) days</i>
GSA0	1.53	1.57	1.81	1.79	2.07	2.13
GSA5	1.57	1.72	1.85	1.94	2.10	2.27
GSA10	1.56	1.68	1.84	1.85	2.08	2.19
GSA15	1.54	1.67	1.82	1.84	2.07	2.17

*Each value actors as the average of three cubic

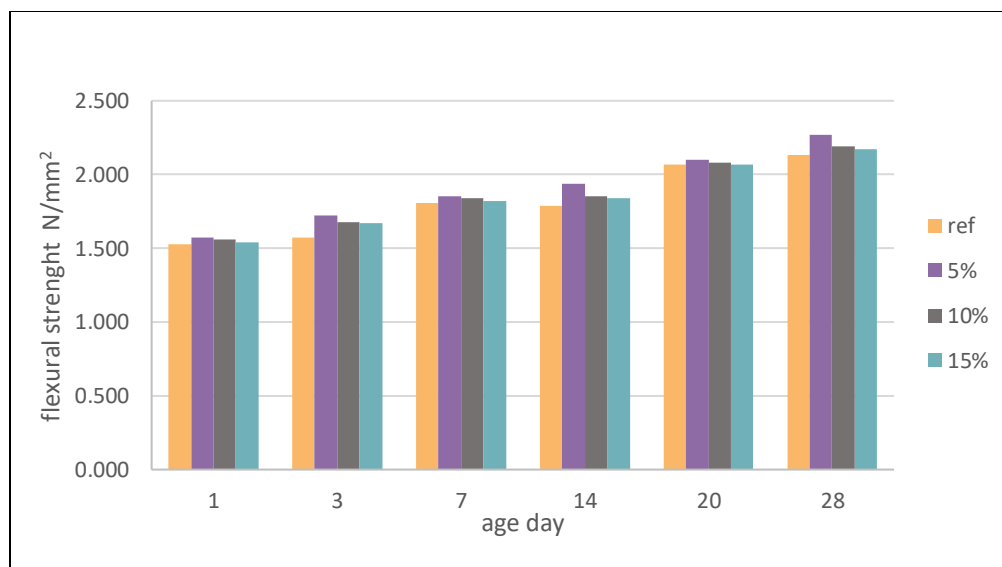


Figure 4-8: Behaviour of flexural strength in grouts with CDWTS at different ages

The trend is similar to the compressive strength. The maximal flexural strength appeared when the CDWTS replaced 5% of the cement, where the flexural strength increases with the age of curing (Demirboğa et al., 2004). As for grout incorporating more than 5 % of the CDWTS content, the flexural strength decreased but was still higher than that of the reference sample. The pozzolanic activity from CDWTS could explain flexural strength.

For GSA5 The percentage of increase in flexural strength of the ages (1,3, and 7) days were 2.6%.9.5%, and 2.2% respectively. With progress age of curing (14,20, and 28) days, the gain rates were 8.8%,1.4, and 6.57 respectively.

For GSA10, the rate of increasing of the early ages were (1.9%,7%, and 1.6%), and for the late ages were (3.3%,0.4%, and 2.8%). Finally, for GSA15, the rates of development were (0.6%,6.3%,0.5%,2.7%,0%, and 1.8%) of all ages.

The CDWTS reacted with CH, which had been generated through cement hydration and formed extra calcium silicate hydrate gel C-S-H in the

binder matrix. Moreover, the dense structure also helps in flexural strength and improves the mechanical performance of the grout. The sludge treatment seems to have a slight effect, not noticeable except for 5% on the enhancement of the flexural strength of CDWTS. These results were in agreement with Duan et al. (2020)

4.7.3 Ultrasonic Pulse Velocity (UPV)

Ultrasonic pulse velocity was assessed on grout prisms to evaluate the regularity of the grout. Table 4-6 and Figure 4-10 show the UPV range for the cement grout mixes with 0%, 5%, 10%, and 15% CDWTS substitution, as well as the curing age for each of these combinations, respectively.

Table 4-6:UPV observed with and without the CDWTS

UPV at various ages (m/s)						
Mix. lab	<i>(1) day</i>	<i>(3) days</i>	<i>(7) days</i>	<i>(14) days</i>	<i>(20) days</i>	<i>(28) days</i>
<i>GSA0</i>	2.652	3.121	3.421	3.519	3.600	3.727
<i>GSA5</i>	2.769	3.464	3.661	3.726	3.821	4.124
<i>GSA10</i>	2.398	2.663	3.206	3.749	3.948	4.300
<i>GSA15</i>	2.281	2.517	3.023	3.786	3.983	4.414

Each value actors as the average of three prisms

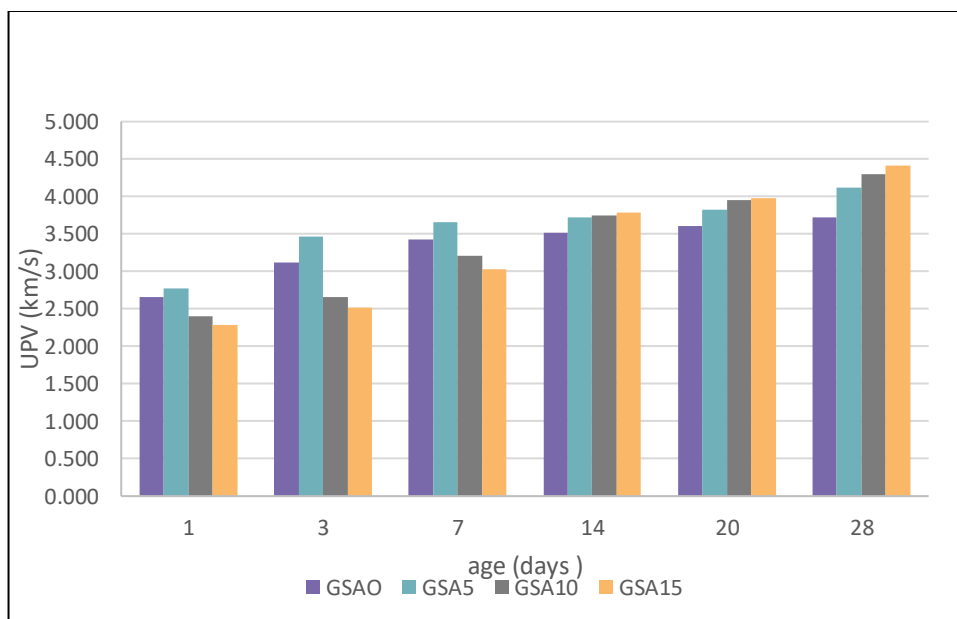


Figure 4-9: Evolution of the ultrasonic pulse velocity of grouts with the age.

The figure shows that the UPV increased with the age of curing for all mixtures. The early stage has higher development in the velocities. However, late ages seem constantly growing in velocities. In the early ages, the UPV is optimum for GSA5 and minimum for GSA15. In contrast, the late ages show a higher enhancement in the velocities for the reference mixture.

Gain rates at 1, 3, and 7 days old are shown to be improved by 4.4%, 10%, and 7%, respectively, using the GSA5. The GSA15 has the lowest reduction in velocity at 14%, 19%, and 11% for ages 1, 3, and 7 days, respectively. The velocities of GSA10-treated samples are lower than those of the reference combination by 9.5%, 14.6%, and 6.2%, respectively, for the same ages. The GSA15 shows increasing velocities of 7.5%, 10.6%, and 18% at 14, 20, and 28 days of curing time, respectively. The GSA10 enhancement in the velocities was 6.5%, 9.6%, and 15% with respect to the control mixture. Furthermore, the GSA5 reveal enhancement in the late age with respect to the control mixture but is lower than the GSA10 and GSA15. The GSA5 is 5.8%,

6.1%, and 1% higher than the control mixture for the ages 14, 20, and 28, respectively.

The development of velocities with age for all mixtures is because the hydration products keep going continuously. Additionally, the density of the grout may be responsible for the rise in UPV with CDWTS's incorporation since ultrasonic travels more freely through thick media than through more porous ones (MERMERDAŞ et al., 2020). Cement grout mixes, including CDWTS, may be placed in a good class in terms of the values supplied in Table 3-5, as seen when comparing the findings to the classifications given in chapter three.

4.7.4 Hardened Density

The measurement of hardened density can measure the durability of hardened grout. The results of water absorption by total immersion of all mixtures measured at 28 days are illustrated in Figure 4-11. It can be seen that the water absorption decreased for grout containing CDWTS from 0% to 15%. The results indicated that the pore size refinement from the pozzolanic reaction of the CDWTS was significant. The reduction in water absorption for grout containing CDWTS is believed to be because of a denser microstructure, which is thought to be due to the improved particle. With more contents of the CDWTS incorporated into the cement, more calcium silicate hydrate gel (C-S-H) could be generated from the pozzolanic reaction between the CDWTS and hydroxide alcalcium (CH). The extra-formed C-S-H may fill the large and open pores, converting them to gel or closed pores, thereby reducing pore connectivity. Interestingly, these results agreed with Duan et al. (2020).

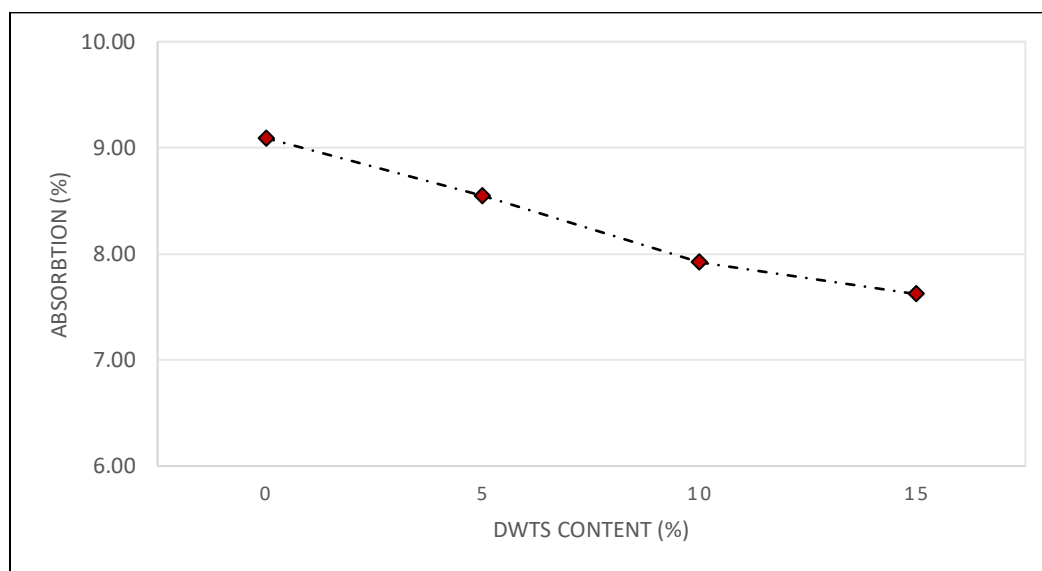


Figure 4-10:Effect of CDWTS on absorption of grout sample

For the packing density and pores, the percentage of the GSA5 that improved is because it is the additive, despite its density, which is less than the density of cement, but the products of the reaction of C-S-H instead of the decrease. For GSA10 and GSA15, the decrease that occurred may be because a heavy material was replaced by a lighter material, and the C-S-H here did not compensate for the decrease in the density that occurred and was not sufficient to fill the pore. Furthermore, the packing density hypothesis states that adding very small particles to a combination with low powder content causes them to fill more spaces, increasing packing density. However, due to specific chemical reactions that decrease the packing density, a reversal behaviour is anticipated with higher doses of very small particles. The presence of too many fine particles causes the particles to push against one another, increasing the void content and lowering the packing density (Kwan and McKinley, 2014).

CDWTS particles result in improved particle packing, resulting in denser cement grout; using CDWTS as a partial replacement for cement also lowers the volume of voids in the cement grout (see Figure 4-11).

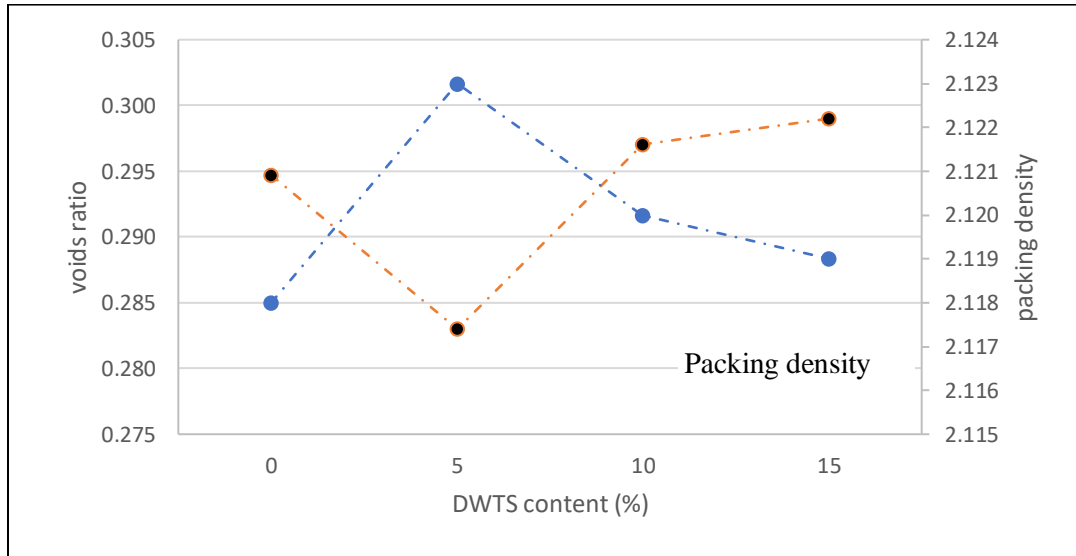


Figure 4-11: Voids Ratio and Packing Density Versus CDWTS Content.

4.8 Microstructural Observation (SEM-EDX)

The data presented in the preceding section relating to the experiment field's results make it abundantly evident that the CDWTS % significantly affects the mechanical, fresh, and durability qualities of cement-based grout. For instance, the compressive strength with 5% CDWTS has improved dramatically. However, 10% and 15% have had less of an impact. This, however, presents the issue of how these percentages work with cement binders to enhance characteristics. The mechanical properties of produced grout are closely related to its internal microstructure.

SEM observation was performed to study the morphology variation of the cement grout after replacing it with CDWTS. On the other hand, EDX is a microanalytical technique based on the detection of X-rays. Figures from 4-

12 to 4-15 show the SEM images of grout samples with CDWTS replacement varying from 0 to 15 %.

The research questions revealed that replacing CDWTS influenced the hydration product and caused significant modifications in the microstructures or morphological forms of the particle's core. Some macro-and micro-pores could be seen within the images in Figure 4-13(a) and (b) of the specimens created using cement, which may have been due to some hydration products, such as the calcium hydroxide $\text{Ca}(\text{OH})_2$. In addition, the microstructure of the control group (GSA0) is quite dense, comprised of platy $\text{Ca}(\text{OH})_2$, fibrillary C-S-H, and needle-like ettringite. Dark zones indicate zones of lower density of hydrates and increased quantity of small pores. This coarse porosity is not observed for specimen GSA5 and GSA10, which show a very homogeneous and dense microstructure. In addition, more compact formation of hydration products and a lesser amount of crystalline components

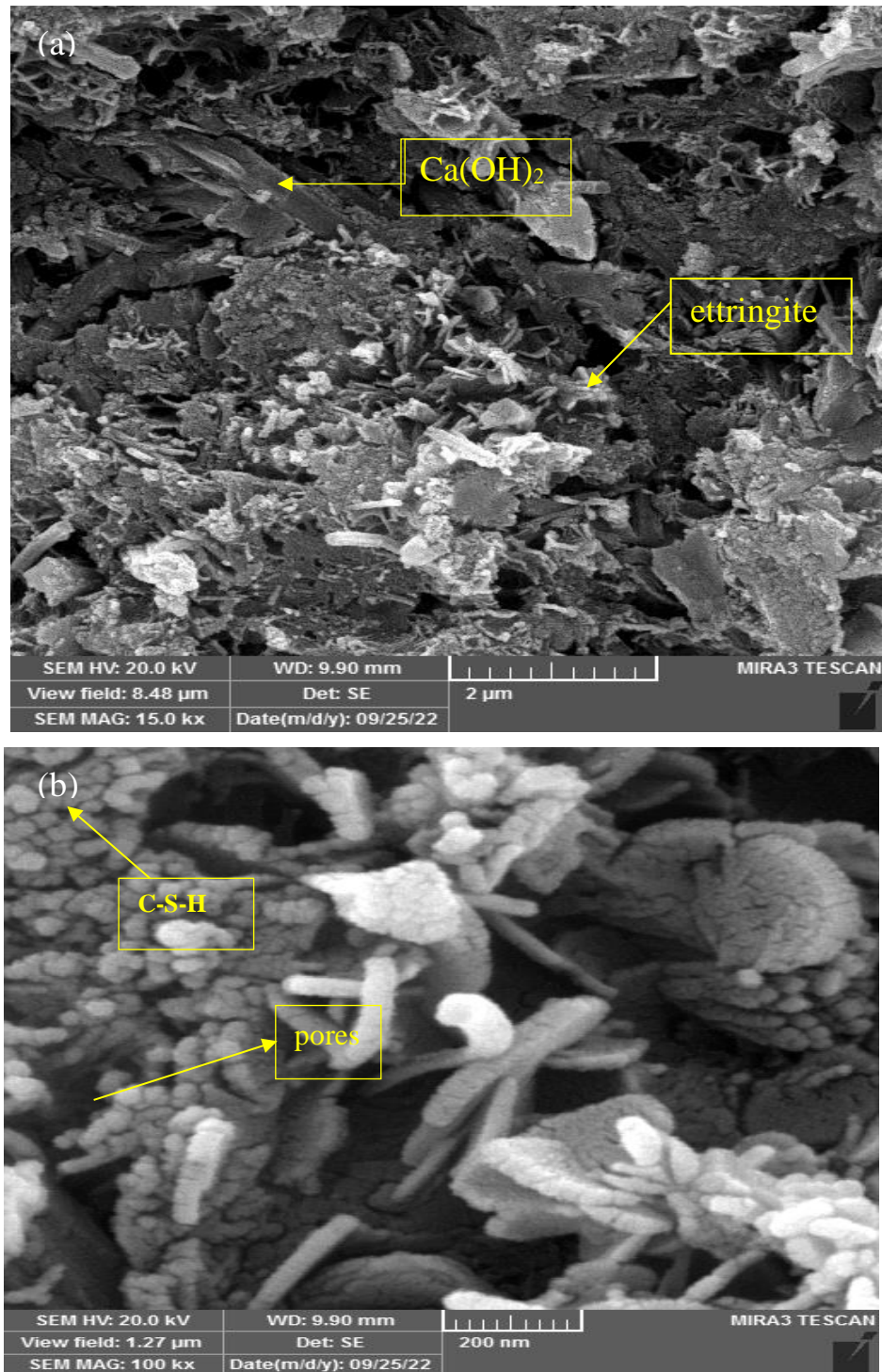


Figure 4-12: SEM observation of cement mixture at 28 days of curing with a) 2μm.b)200nm

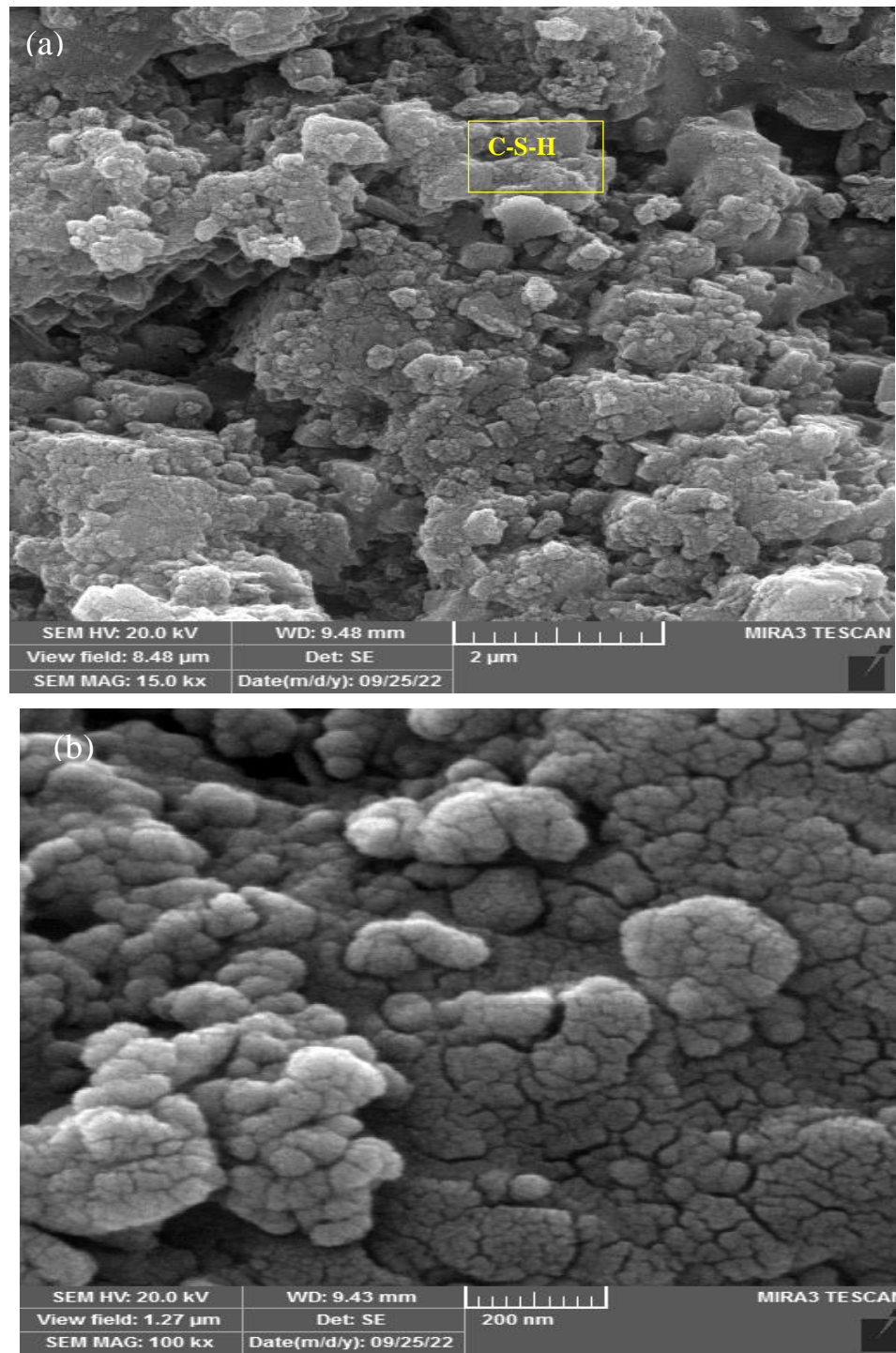


Figure 4-13: SEM observation of GSA5 mixture at 28 days of curing with a) $2\mu\text{m}$. b) 200nm

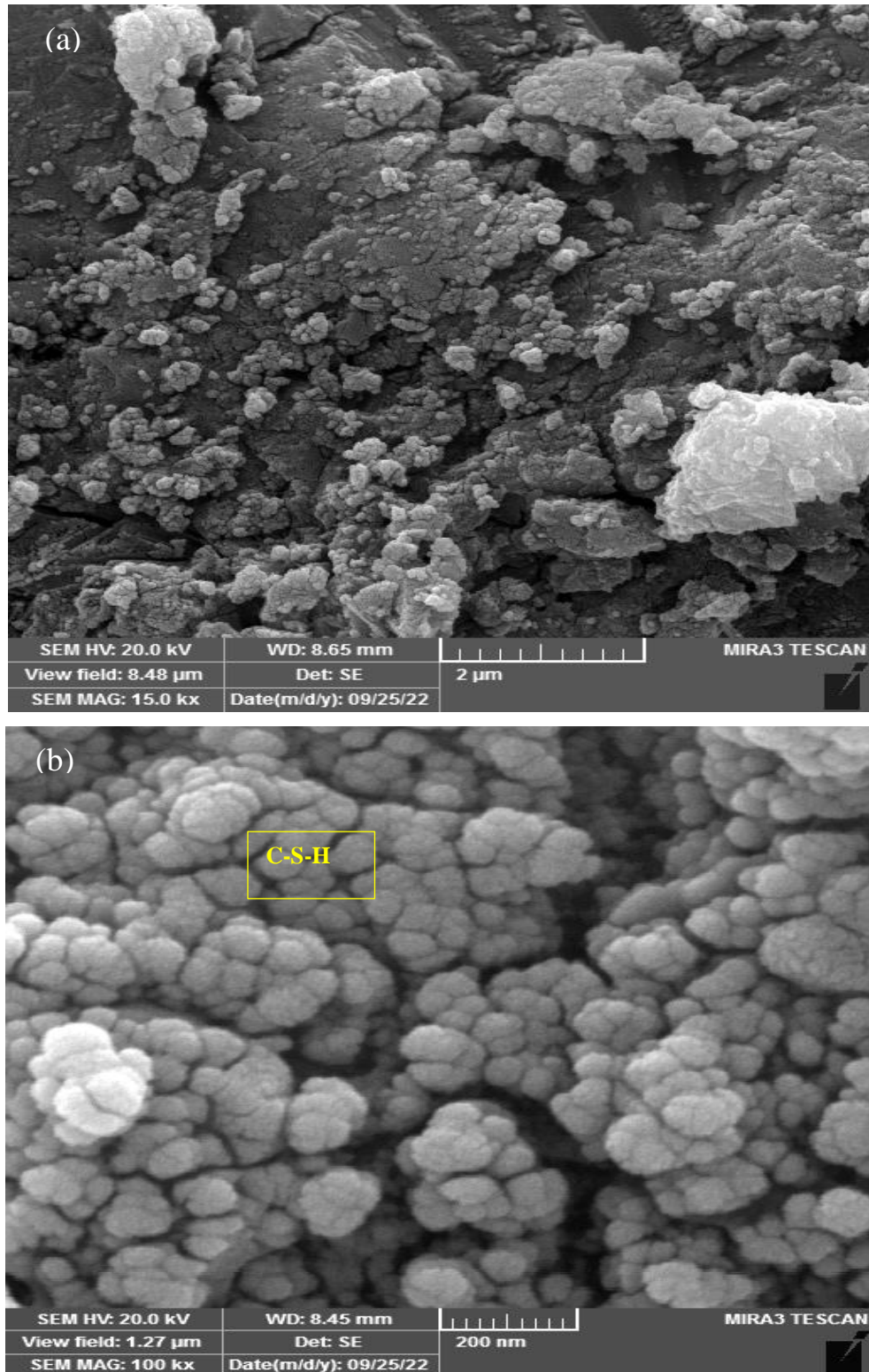


Figure 4-14: SEM Observation of GSA10 Mixture at 28 days of curing with a) 2μm.b)200nm

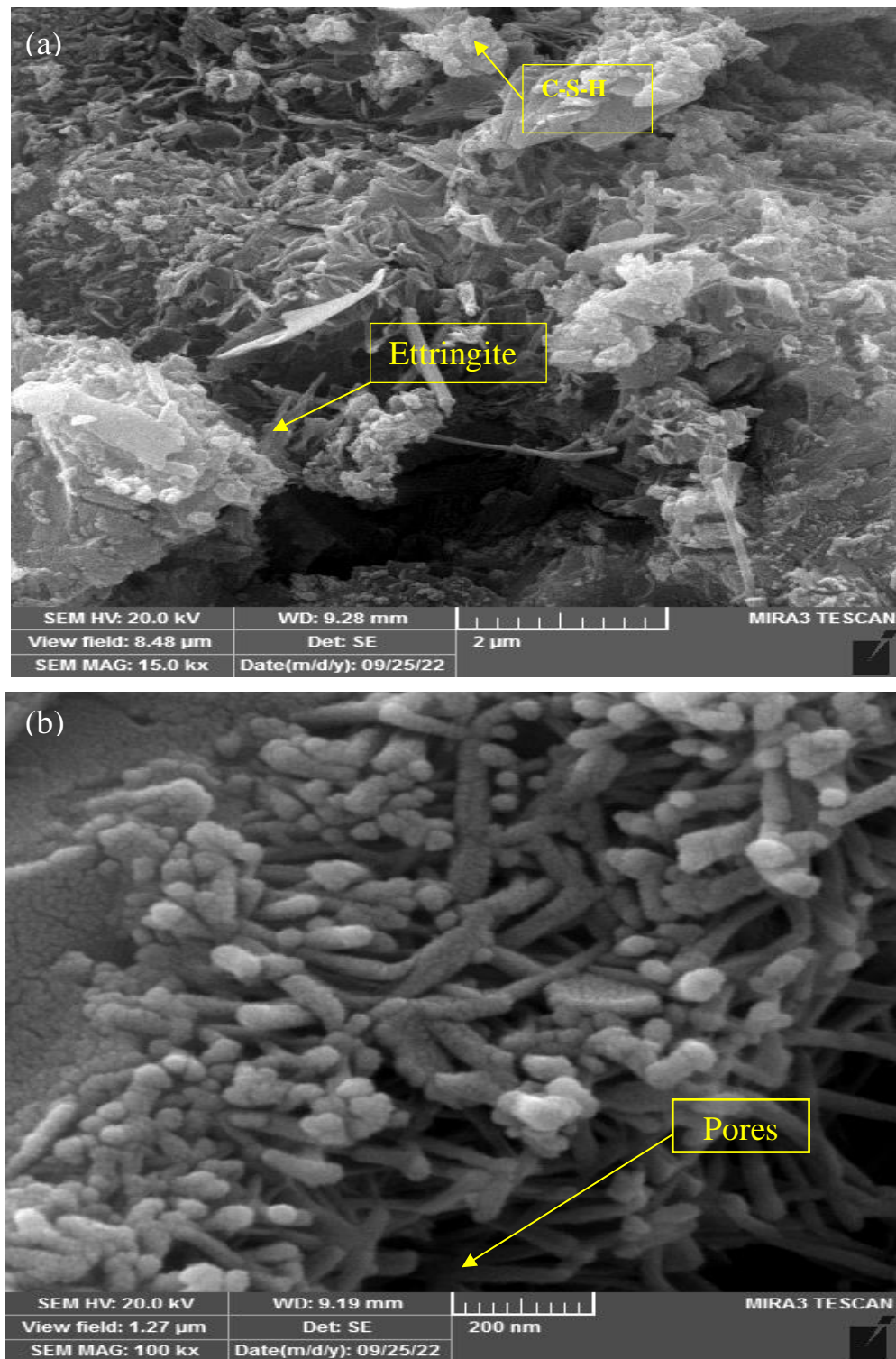


Figure 4-15: SEM Observation of GSA15 Mixture at 28 days of curing with a) 2 μm .b)200nm

The predominant compound in GSA5, and GSA10 was the interwoven cotton-shape (C-S-H) calcium silicate hydrate gel as illustrated in Figure 4-13 (a), and Figure 4-14 (a), which are the major hydration by-product of Portland cement and the filling effect was due to pozzolanic activity of CDWTS.

The pore space aperture between the particles became narrower or negligible and dense packing of the mixture with 5% and 10% replacement of cement. Physically, the small fineness of the CDWTS particles allows them to fill holes and splits while enhancing pore structure. This result and the discovery that the pozzolanic reaction between Portlandite and CDWTS generated a thick texture (Figure 4-13 (b): Figure 4-14(b)) leading to the mixture's high strength.

However, its effects on modifying the microstructure are reversed when the replacement rate of CDWTS is too high. The specimens GSA15 have fewer hydration products and a looser microstructure. Some holes can be seen in the matrix (Figure 4-15 (a)), which is another saying that some anhydrate CDWTS particles are beginning to form. This may happen due to the rate of pozzolanic reactions, which consumed all of the portlandite, and where CDWTS would be present in the cementitious matrix as an inert phase. These factors can explain this decline. Reduced contact area and delayed slurry setting result from the development of needle-like AFt coating on the surface of the materials (Figure 4-15 b). While this is occurring, the volume expansion provided by the formation of AFt compensates for its drying shrinkage during the hydration phase.

SEM-EDX analysis was then used to determine the elemental composition of the C-S-H. In the EDX spectrums, Figure 4-16 showed that the element concentration varied for the GSA0, GSA5, GSA10, and GSA15. The GSA5 showed the highest peak, which confirmed the SEM result. In addition, the materials were composed of similar elements, namely calcium and silicon.

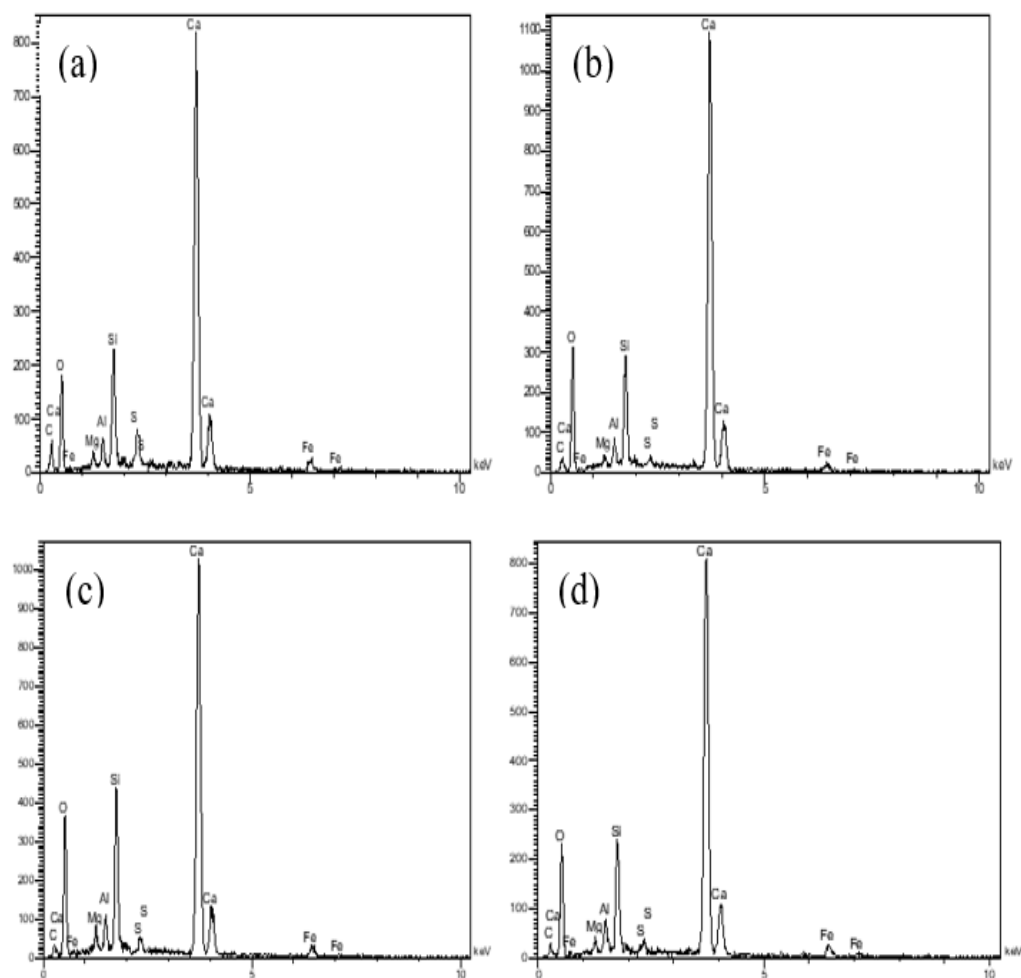


Figure 4-16: Energy Dispersive Analysis with X-Ray of Grout; (A) Neat Cement; (B) 5% CDWTS (C) 10 % CDWTS; (D) 15 %, Showing the elemental peaks of each material.

The EDS analysis also showed some alum contents in the cement matrix of the treated CDWTS-modified grout, which indicated that treated CDWTS was presented in the cement matrix, probably because the thinnest ash particles had similar characteristics as cement particles. The C, O, Si and Ca peaks in the EDS result confirmed the presence of C-S-H and CaCO₃. Moreover, more details can be detected but, due to limited time and resource enough with that explanation. However, the dominant compound in the GSA SEM image was the cotton-shaped C-S-H gel, which was the main product of the cement hydration reaction. Although the cubic-shaped crystalline CaCO₃ was also observed.

Chapter Five : Statistical Modelling

5.1 Soft Computing Technique and Statistical Modelling

5.1.1 General

In addition to being quicker, statistical modelling offers an advantage over competing methods since it allows for the definition of confidence intervals for forecasts and is theoretically sound. This is especially evident when approaches based on artificial intelligence are contrasted with statistical modelling. Through correlation analysis, statistical analysis may also provide light on the main elements affecting compressive strength. Statistical modelling is advantageous over other methods because it is quick and can create forecast confidence ranges. It also has the advantage of being mathematically sound. This is especially evident when approaches

An overview of the theoretical aspects of regression and correlation analysis is provided in the subsequent sections. In the following, MLR models were performed by the statistical package for social (SPSS) software (version 26). Using regression and correlation techniques, the relationships between variables demonstrate how to identify their kind and degree. Based on previous observations of the unknown variable and other relevant variables, it will be feasible to forecast the value of an unknown variable with some accuracy. Sir Francis Galton introduced regression as a statistical concept in 1887. Regression is the name has given to the broad process of extrapolating one variable from another.

Later, statisticians created the phrase "multiple regression" to characterize the method of using many variables to predict another. Regression analysis generates an estimating equation, a mathematical formula that correlates a known variable to an unknown variable. Only one dependent variable can be predicted or estimated in a regression analysis. Although more than one independent variable can be utilized for analysis, employing more than

one input will only allow to predict a single result at most. In general, increasing the inputs improves forecast accuracy (Independent variable). It is common for a causal link to form, meaning that the independent variable "causes" the dependent variable to change. However, in many instances, a different factor is what alters both the dependent and independent variables. It is crucial to remember that the links shown by the regression are ties of association rather than necessarily ones of cause and effect. The analysis may only be partially complete unless there are particular grounds for thinking that the dependent variable's (s) values are determined by the independent variable's (s) values.

5.1.2 Multiple Linear Regression (MLR)

MLR is commonly used to estimate compressive strength due to its simple methods and theory (Khademi and Jamal, 2017). In these methods, the training dataset is used to fit a linear equation that models the relation between various IVs and a DV, as shown in eq 5-1:

$$\hat{Y} = B_0 + \sum_{i=1}^n B_i X_i + \varepsilon \quad \text{Eq 5-1}$$

Where:

\hat{Y} is the expected outcomes value DV.

ε is the random residual error coefficient.

x_i (1, 2, ..., n) are the IVs.

B_i (1, 2, ..., n) are the regression coefficients.

Compressive strength is a function of several parameters, including (age and solid material content) which can be expressed as follows:

$$c.s = f(\text{age}, \text{solid content}) \quad \text{Eq 5-2}$$

The objective is to estimate compressive strength, flexural strength, and ultrasonic pulse velocity using curing age and cementitious solid content. Thus, parameters, namely compressive strength (measured by Mpa) (CS), flexural strength (measured by Mpa) (F.S), ultrasonic pulse velocity (measured by m/sec) (UPV), age (day), (solid content %). Therefore, the other parameter is expressed by the following equation:

$$F.S = f(\text{age, solid content}) \quad \text{Eq 5-3}$$

$$UPV = f(\text{age, solid content}) \quad \text{Eq 5-4}$$

According to the above assumptions, it is important to describe the r square in a statistically significant manner to create MLR models (Abdulredha et al., 2018). The regression coefficients can be calculated using standard, hierarchical, and stepwise approaches. Due to its capacity to include the IVs effect correlations with the DV in the current investigation, an entry MLR approach was used. Two steps must be taken to generate an entry MLR. The first step is to confirm the method and data processing assumptions, and the second is to assess the effectiveness of the created model and the role of IVs.

5.1.3 MLR Assumption

5.1.3.1 Variables Types

One of the study design's critical parts is the variable's nature. Different variables, including continuous and categorical ones, are assessed at various levels. Weight is one example of a continuous scale variable that is measured (measured in kg) (Statistics, 2015). A variable with a categorical component has a limited set of potential values.

Nominal and ordinal variables are examples of categorical data. In contrast to ordinal categorical variables whose possible values are sorted in a definite order, such as education level, the nominal categorical variables like gender have two or more categories but no natural ordering. The DV in an MLR analysis should be a continuous scale variable, and the IVs should contain at least two continuous or nominal-level measurements (Pallant, 2020). Moreover, the ordinal variable must be represented as a nominal or continuous level to be inserted into an MLR (Statistics, 2015)

5.1.3.2 Sample Size

The dataset's size impacts how generally applicable the MLR model is because results from a small dataset cannot be applied (Pallant, 2020). The following equation may be used to determine the minimal sample size needed to create a generalizable model while accounting for the quantity of IVs (Tabachnick and Fidell, 2013):

$$N \geq 50 + 8 * n \quad \text{Eq 5-5}$$

Where: N is the sample size.

n is the number of explanatory IVs used in the MLR.

5.1.3.3 Normality of IVs and DV

Variable normal testing is a crucial preliminary step in MLR. Even if the normality of IVs is not always necessary for data analysis, the outcome is more reliable if all IVs are distributed properly (Tabachnick and Fidell, 2013). Q-Q plots, or expected normal probability plots, are useful graphical tools for determining normality (Kern et al., 2015). These charts compare each case's actual and predicted normal values. The more closely the actual values follow a normal distribution, the more closely they resemble the predicted values

(Tabachnick and Fidell, 2013). To improve the distribution of variables, the literature offers a variety of data transformation techniques, such as logarithmic transformations, depending on the direction of the skewness and the extent of a normal distribution (Tabachnick and Fidell, 2013).

5.1.3.4 Linearity of IVs

This phrase describes the relationship between DV and IVs. It is necessary to independently and together test this premise (Pallant, 2020, Tabachnick and Fidell, 2013). Partial regression graphs between the DV and each IV or univariate scatter plots for all variables may be used to test the hypothesis that the DV and each IV are linearly related to one another (Statistics, 2015). To be clear, evaluating the linearity is optional at this stage. Thus, categorical variables like education level may be disregarded (Statistics, 2015). This all assumes that the relationship between the DV and IVs is linear. Plotting a scatterplot of the standardized residuals versus the (unstandardized) projected value will verify this assumption (Statistics, 2015). This assumption must be met for the standardized residuals to generally form a rectangle distribution, with most of the observations centred on the plot (Statistics, 2015).

5.1.3.5 Residuals Homoscedasticity

It is assumed by homoscedasticity that residuals are constant throughout a range of DV expectations (Pallant, 2020, Tabachnick and Fidell, 2013). This indicates that the DV's value does not affect the residual readings. This assumption may be verified using the same plot of the standardized residuals vs the (unstandardized) expected values. It is possible to verify this assumption when the residual variances follow a roughly rectangular distribution and the residuals do not show any blatant systematic patterns, such as being curved or larger on one side than the other (Tabachnick and Fidell, 2013).

5.1.3.6 Observations Independence

MLR assumes that any adjacent two instances' errors are uncorrelated (Statistics, 2015). This assumption is incorrect when the residual terms are correlated (Abdulredha et al., 2018). The residual serial correlation Durbin-Watson test may be used to check this assumption (Tabachnick and Fidell, 2013). The closest value to 2 on the Durbin-Watson test's scale of 0 to 4 indicates that the residuals are uncorrelated (Abdulredha et al., 2018).

5.1.3.7 Absence of Outliers

A case with a unique value or one that opposes other cases in the same variable is an outlier (Tabachnick and Fidell, 2013). Outliers skew conclusions and reject the regression outcome, negatively impacting the findings made from MLR. consequently, IVs and DVs must be analyzed to avoid such high values in the first screening runs (Statistics, 2015). It is possible or unlikely that cases with standardized residuals larger than 3 are reflective of an outlier. Statistically, the Mahalanobis distances may determine whether any variables contain outliers (Pallant, 2020). The latter values must be less than the critical values (Tabachnick and Fidell, 2013)

5.1.3.8 Multicollinearity

Multicollinearity is a phenomenon where the IVs in the data set correlate, which negatively impacts the MLR result (Pallant, 2020). One of the correlated IVs must be reduced to solve multicollinearity, or a new IV must be created to represent the connected IVs (Statistics, 2015). The Variance Inflation Factor (VIF) statistics can be used to determine the presence of multicollinearity (Equation (3-14)) by which each IV, represented by U , becomes the response DV, while the other IVs are preserved as independent variables. Accordingly, the VIF is determined for each IV (VIF_U) as in (Tabachnick and Fidell, 2013). The current literature provides a wide range of threshold values for VIFs. A

value of more than 10 is a common cut-off point in the literature used to confirm the existence of multicollinearity in this dataset.

$$VIFU = \frac{1}{1 - R^2} \quad \text{Eq 5-6}$$

Where: VIF is the Variance Inflation Factor value.

R^2 is the regression coefficient of determination for the U explanatory variable.

5.1.3.9 Contribution of IVs.

According to their statistical significance (p), the impact of IVs on the final model findings ranges from noticeable to insignificant (Tabachnick and Fidell, 2013). The proposed model is very sensitive to any variables having P-values below 0.05. Because of their negligible effect on the model, variables with p-values over 0.05 are considered significant (Pallant, 2020).

A leading factor of the MLR model's success is its predictive accuracy, or capacity to account for deviations in the DV (Statistics, 2015). The R^2 is a useful statistic for evaluating the accuracy of a model's predictions by comparing actual results to those generated by the model. Coefficients of 1 or closer (determined using equation (3-15)) indicate that the model may provide a valid result (Tabachnick and Fidell, 2013).

$$R^2 = \frac{\hat{y}}{y} \quad \text{Eq 5-7}$$

When Y is the total squared difference between the mean and the observed scores, Y' is the total squared difference between the mean and the predicted scores.

Working with a limited amount of data, the calculated R^2 value is sometimes too optimistic (Tabachnick and Fidell, 2013). The Adjusted R^2 (calculated based on Eq 3-16), which considers both the data set's size and the number of predictive variables, offers a more accurate assessment of the model (Statistics, 2015).

$$adjusted R^2 = 1 - (1 - R^2) \left(\frac{1 - N}{1 - n - N} \right) \quad \text{Eq 5-8}$$

Where:

N represents the number of observations.

n represents the number of variables.

5.2 Result of Statistical Analysis

With the use of a statistical software application, the data were examined. Multi-linear regression analysis was used to find the model coefficients, which are presumed to be normally distributed. Given that the error was thought to be random and regularly distributed, it stands to reason that the residual terms which indicate the discrepancy between the actual and anticipated values would also have similar characteristics. All components and interactions are evaluated for statistical significance using the probability value (Prob.) derived from the ANOVA table. The likelihood that the estimated coefficients of the different factors in this study affected each answer was limited to 5% for the majority of the parameters. This constraint indicates that there is less than a 5% probability (or a 95% confidence limit) that the contribution of a certain parameter to the tested response will be greater than the value of the designated coefficient.

5.2.1 Results of the Compressive Strength Production Model

The correlation matrix between the variables in the regression model is tabulated in table 5-1. Age and compressive strength had the strongest correlation coefficients, with a significant value of 0.00. With a Pearson

correlation of just 0.083 out of a significant 0.243, it is clear that the mixture does not affect the growth of compressive strength. This supports our claim that the CDWTS has significant characteristics and can act as cementitious materials in grout development.

Table 5-1: Table of correlation analysis among influencing factors of compressive strength

		CS	Mix	Age
Pearson Correlation	CS	1.000	.083	.770
	Mix	.083	1.000	.000
	Age	.770	.000	1.000
Sig. (1-tailed)	CS	.	.243	.000
	Mix	.243	.	.500
	Age	.000	.500	.

Table 5-2 shows the model summary. It can be seen that the determination coefficient is 0.599, suggesting that the developed model is able to estimate about 60% of the variation in the compressive strength based on the variation in the age and mixture of the cubs.

Table 5-2: Model Summary of compressive strength

Model	R	R Square	Adjusted R Square	Std. Error of the Estimate	Change Statistics					Durbin-Watson
					R Square Change	F Change	df1	df2	Sig. F Change	
1	.774 ^a	.599	.588	5.92324	.599	51.610	2	69	.000	.583

The results of the ANOVA analysis used to determine the significance of the regression are shown in Table 5-3. The value of sig is 0.000, which is less than 0.01. Therefore, researchers accept the alternative hypothesis that the regression is significant, suggesting that the independent factors affect the dependent variable and that the dependent variable can be predicted using these independent variables.

Table 5-3: Analysis of Variance of compressive strength

Model		Sum of Squares	Df	Mean Square	F	Sig.
1	Regression	3621.457	2	1810.728	51.610	.000 ^b
	Residual	2420.850	69	35.085		
	Total	6042.307	71			

The degree of multicollinearity was evaluated using the variance inflation factor (VIF) and tolerance in addition to the baseline assumptions. As a general rule, strong multicollinearity is signified by a variable with a VIF value larger than five or a tolerance lower than 0.2 (Sahoo and Jha, 2015). Table 5-4 summarizes the findings of the multicollinearity check using the standard method, which showed no multicollinearity because the magnitude of the VIF is less than five. The tolerance is more significant than 0.2 for all independent variables (compressive strength) used in the regression model.

Table 5-4: Regression Coefficients Values of compressive strength

Model		Unstandardized Coefficients		Standardized Coefficients	T	Sig.	95.0% Confidence Interval for B		Correlations			Collinearity Statistics		
		B	Std. Error	Beta			Lower Bound	Upper Bound	Zero-order	Partial	Part	Tolerance	VIF	
1	(Constant)	13.865	1.466		9.456	.000	10.940	16.791						
	Mix	.137	.125	.083	1.095	.277	-.112	.386	.083	.131	.083	1.000	1.000	
	Age	.736	.073	.770	10.101	.000	.591	.881	.770	.772	.770	1.000	1.000	

Table 5-4 also displays the design parameters. Using these numbers, one may devise a regression equation to foretell the extraction efficiency given the relevant data. The coefficients table provides information on how each independent variable affected the final linear regression, as Abdulredha et al. (2018) stated. Each constraint's relative importance to the overall results of the analysis model has discussed in the significant (sig) column. Moreover, the

table shows that age has a significance level (sig) lower than 0.05. These results support that age has a significant role in the model's predictions.

However, the p value is above 0.05, suggesting that it does not significantly affect the results of the developed model. This provides evidence for the claim that the compressive strength of the resulting grout is unaffected by the addition of extra CDWTS. This suggests that the CDWTS may serve as an alternative to cement in grout development.

Probability and histograms of residuals were used to verify the normality assumption, respectively. A histogram of residuals with a normal curve overlay is shown in Figure 5-1. The residuals in this plot follow a normal distribution, as seen in the figure.

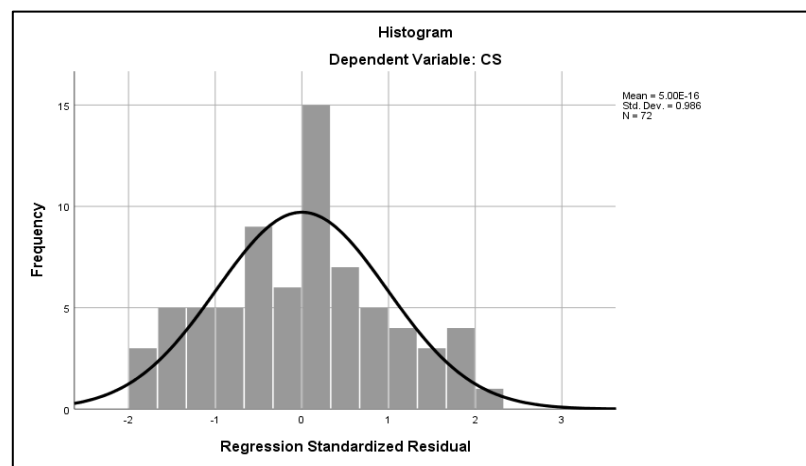


Figure 5-1: Probability Curve for Experimental Curve

Figure 5-2 depicts a normal probability plot of the residuals, which may be used to assess whether or not the residuals can be assumed to follow a normal distribution and, potentially, to identify outliers. Since the majority of residuals lie on a straight line in the normal probability plots of residuals shown in the preceding image, this proves that the residuals collected follow a normal distribution.

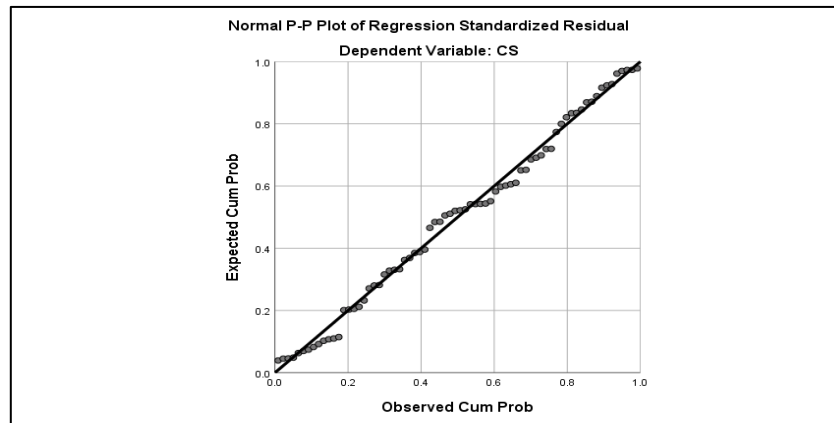


Figure 5-2: Linear Probability of Predicted Compressive Strength

Figure 5-3 displays graphs of the standardised residuals (errors) and predicted values of *cs*, which may be used to test the homoscedasticity assumption. The residuals represent the discrepancy between observed data and predicted values. These residuals are excellent for spotting irregularities. As seen in Figure 5-3, None of the residuals stands out significantly from the rest, and the pattern overall seems random. None of the residuals had Studentized values of three or less. There are also no out-of-the-ordinary residuals in this model.

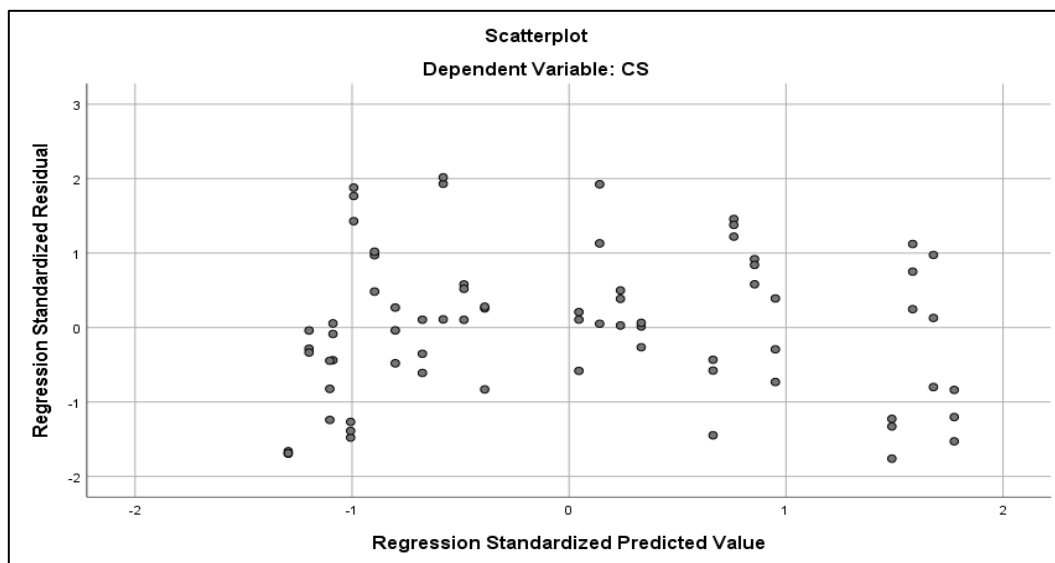


Figure 5-3: Scatter Plot of compressive strength

5.2.2 Results of the Ultrasonic Pulse Velocity Prediction Mode

The correlation matrix between the variables in the regression model is tabulated in Table 5-5. Age and UPV had the strongest correlation coefficients, with a significant value of 0.00. With a Pearson correlation of just -0.096 out of a significant 0.212, it is clear that the mixture does not affect the growth of compressive strength. This supports our claim that the CDWTS has significant characteristics and can act as cementitious materials in grout development.

Table 5-5: Table of correlation analysis among influencing factors of ultrasonic pulse velocity

Correlations				
		UPV	Mix	Age
Pearson Correlation	UPV	1.000	-.096	.866
	Mix	-.096	1.000	.000
	Age	.866	.000	1.000
Sig. (1-tailed)	UPV	.	.212	.000
	Mix	.212	.	.500
	Age	.000	.500	.
N	UPV	72	72	72
	Mix	72	72	72
	Age	72	72	72

Table 5-6 shows the model summary. It can be seen that the determination coefficient is 0.759, suggesting that the developed model is able to estimate about 76% of the variation in the compressive strength based on the variation in the age and mixture of the cubs.

Table 5-6: Model Summary of ultrasonic pulse velocity

Model Summary ^b										
Model	R	R Square	Adjusted R Square	Std. Error of the Estimate	Change Statistics					Durbin-Watson
					R Square Change	F Change	df1	df2	Sig. F Change	
1	.871 ^a	.759	.752	.30024	.759	108.694	2	69	.000	.517

a. Predictors: (Constant), age, mix

b. Dependent Variable: UPV

The results of the ANOVA analysis used to determine the significance of the regression are shown in Table 5-7. The value of sig is 0.000, which is less than 0.01. Therefore, researchers accept the alternative hypothesis that the regression is significant, suggesting that the independent factors affect the dependent variable and that the dependent variable can be predicted using these independent variables.

Table 5-7: Analysis of Variance for ultrasonic pulse velocity

ANOVA ^a						
Model		Sum of Squares	Df	Mean Square	F	Sig.
1	Regression	19.597	2	9.798	108.694	.000 ^b
	Residual	6.220	69	.090		
	Total	25.817	71			
a. Dependent Variable: UPV						
b. Predictors: (Constant), age, mix						

The degree of multicollinearity was evaluated using the variance inflation factor (VIF) and tolerance in addition to the baseline assumptions. As a general rule, strong multicollinearity is signified by a variable with a VIF value larger than five or a tolerance lower than 0.2 (Sahoo and Jha, 2015). Table 5-8 summarizes the findings of the multicollinearity check using the standard method, which showed no multicollinearity because the magnitude of the VIF is less than five. The tolerance is more significant than 0.2 for all independent variables (UPV) used in the regression model. Additionally, the table shows Therefore, getting the regression line's equation for predicted values is supported by the standard and non-standard regression coefficients, the standard error, and the statistical significance of the t-test .

Table 5-8: Regression Coefficients Values of ultrasonic pulse velocity

Coefficients ^a													
Model		Unstandardized Coefficients		Standardized Coefficients	T	Sig.	95.0% Confidence Interval for B		Correlations			Collinearity Statistics	
		B	Std. Error	Beta			Lower Bound	Upper Bound	Zero-order	Partial	Part	Tolerance	VIF
		1	(Constant)	2.809			.074		37.794	.000	2.661	2.957	
	Mix	-.010	.006	-.096	-1.620	.110	-.023	.002	-.096	-.191	-.096	1.000	1.000
	Age	.054	.004	.866	14.655	.000	.047	.061	.866	.870	.866	1.000	1.000

a. Dependent Variable: UPV

Probability and histograms of residuals were used to verify the normality assumption, respectively. A histogram of residuals with a normal curve overlay is shown in Figure 5-4. The residuals in this plot follow a normal distribution, as seen in the figure.

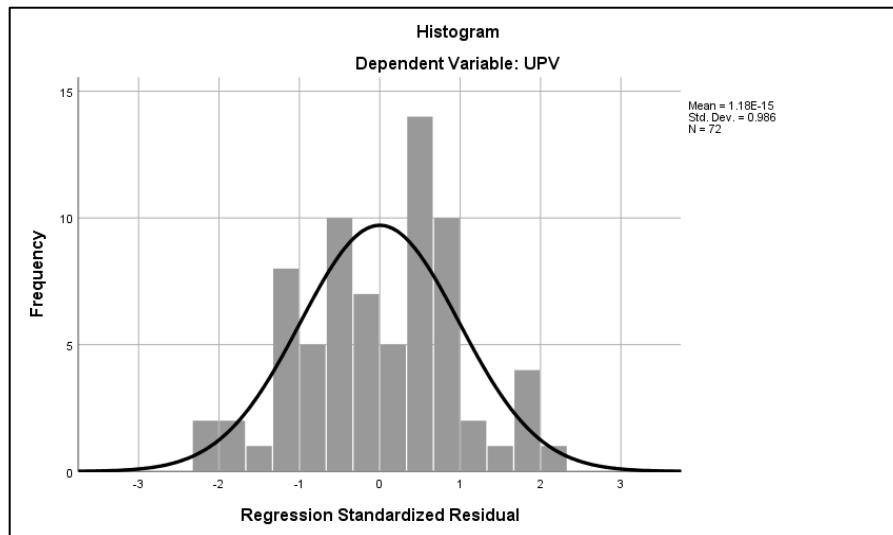


Figure 5-4: Standardized Residuals Histogram of ultrasonic pulse velocity

Figure 5-5 depicts a normal probability plot of the residuals, which may be used to assess whether or not the residuals can be assumed to follow a normal distribution and, potentially, to identify outliers. Since the majority of residuals lie on a straight line in the normal probability plots of residuals shown in the preceding image, this proves that the residuals collected follow a normal distribution.

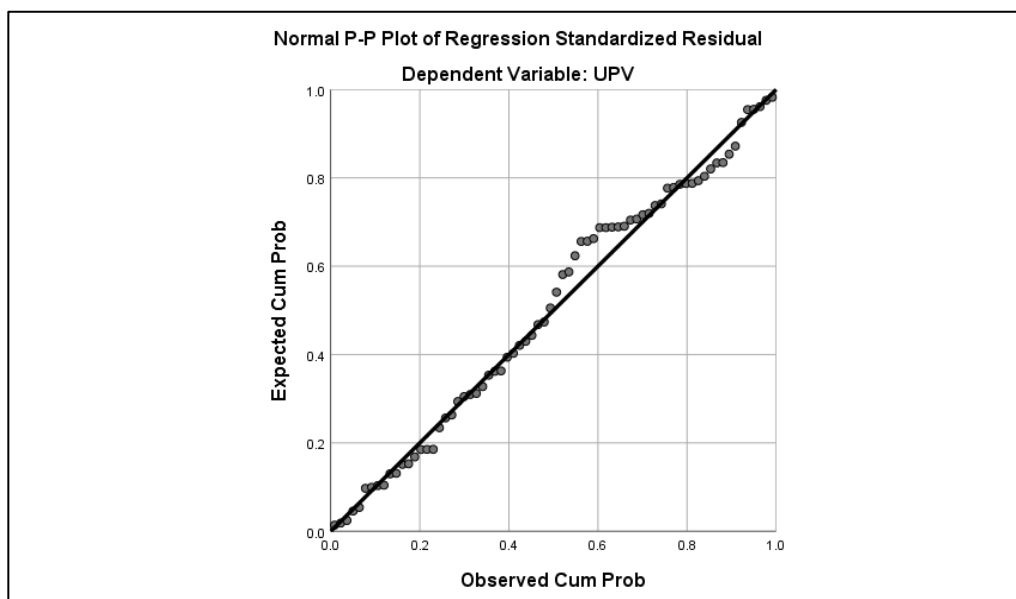


Figure 5-5: The Standardized Residual Normal P-P of ultrasonic pulse velocity

Figure 5-6 displays graphs of the standardised residuals (errors) and predicted values of UPV, which may be used to test the homoscedasticity assumption. The residuals represent the discrepancy between observed data and predicted values. These residuals are excellent for spotting irregularities. As seen in Figure 5-6, None of the residuals stands out significantly from the rest, and the pattern overall seems random. None of the residuals had Studentized values of three or less. There are also no out-of-the-ordinary residuals in this model.

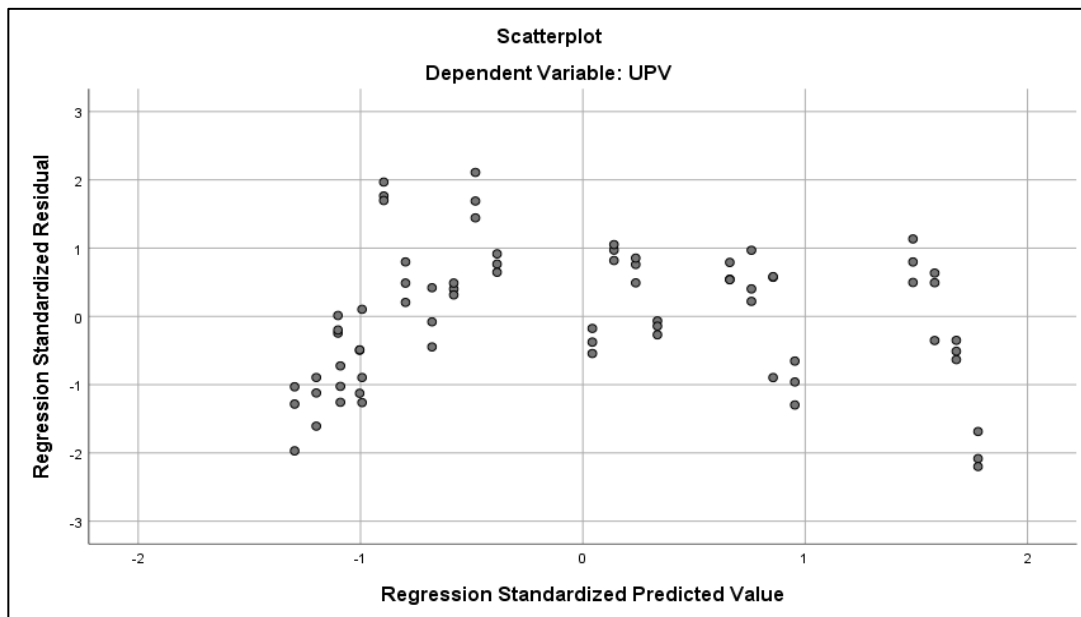


Figure 5-6:Scatter Plot of UPV

5.2.3 Results of the Flexural Strength Prediction Model

The correlation matrix between the variables in the regression model is tabulated in Table 5-9. Age and compressive strength had the strongest correlation coefficients, with a significant value of 0.00. With a Pearson correlation of just 0.019 out of a significant 0.438, it is clear that the mixture does not affect the growth of compressive strength. This supports our claim that

the CDWTS has significant characteristics and can act as cementitious materials in grout development.

Table 5-9: Table of correlation analysis among influencing factors of flexural strength

Correlations				
		F.s	Mix	Age
Pearson Correlation	F. S	1.000	.019	.925
	Mix	.019	1.000	.000
	Age	.925	.000	1.000
Sig. (1-tailed)	F. S	.	.438	.000
	Mix	.438	.	.500
	Age	.000	.500	.
N	F. S	72	72	72
	Mix	72	72	72
	Age	72	72	72

Table 5-10 shows the model summary. It can be seen that the determination coefficient is 0.856, suggesting that the developed model is able to estimate about 85% of the variation in the flexural strength based on the variation in the age and mixture of the cubes.

Table 5-10: Model Summary of flexural strength

Model Summary ^b										
Model	R	R Square	Adjusted R Square	Std. Error of the Estimate	Change Statistics					Durbin-Watson
					R Square Change	F Change	df1	df2	Sig. F Change	
1	.925 ^a	.856	.852	.08810	.856	205.866	2	69	.000	1.618
a. Predictors: (Constant), age, mix										
b. Dependent Variable: F. S										

The results of the ANOVA analysis used to determine the significance of the regression are presented in Table 5-11. The value of sig is 0.000, which is less than 0.01. Therefore, researchers accept the alternative hypothesis that the

regression is significant, suggesting that the independent factors affect the dependent variable and that the dependent variable can be predicted using these independent variables

Table 5-11: Analysis of Variance of flexural strength

ANOVA ^a						
Model		Sum of Squares	Df	Mean Square	F	Sig.
1	Regression	3.196	2	1.598	205.866	.000 ^b
	Residual	.536	69	.008		
	Total	3.731	71			
a. Dependent Variable: F. S						
b. Predictors: (Constant), age, mix						

As mentioned earlier, the degree of multicollinearity could evaluate using the variance inflation factor (VIF) and tolerance in addition to the baseline assumptions. As a general rule, strong multicollinearity is signified by a variable with a VIF value larger than five or a tolerance lower than 0.2 (Sahoo and Jha, 2015). Table 5-12 summarizes the findings of the multicollinearity check using the standard method, which revealed no multicollinearity because the magnitude of the VIF is less than five. The tolerance is more significant than 0.2 for all independent variables (flexural strength) used in the regression model based

Table 5-12:Regression Coefficient Value of flexural strength

Coefficients ^a													
Model		Unstandardized Coefficients		Standardized Coefficients	T	Sig.	95.0% Confidence Interval for B		Correlations			Collinearity Statistics	
		B	Std. Error	Beta			Lower Bound	Upper Bound	Zero-order	Partial	Part	Tolerance	VIF
		1	(Constant)	.558			.022		25.603	.000	.515	.602	
	Mix	.001	.002	.019	.409	.684	-.003	.004	.019	.049	.019	1.000	1.000
	Age	.022	.001	.925	20.287	.000	.020	.024	.925	.925	.925	1.000	1.000

a. Dependent Variable: F. S

Table 5-12 also displays the design parameters. Using these numbers, one may devise a regression equation to foretell the extraction efficiency given the relevant data. The coefficients table provides information on how each independent variable affected the final linear regression, as Abdulredha et al. (2018) stated. Each constraint's relative importance to the overall results of the analysis model has discussed in the significant (sig) column. Moreover, the table shows that age has a significance level (sig) lower than 0.05. These results support that age has a significant role in the model's predictions.

However, the p value is above 0.05, suggesting that it does not significantly affect the results of the developed model. This provides evidence for the claim that the compressive strength of the resulting grout is unaffected by the addition of extra CDWTS. This suggests that the CDWTS may serve as an alternative to cement in grout development.

Probability and histograms of residuals were used to verify the normality assumption, respectively. A histogram of residuals with a normal curve overlay is shown in Figure 5-7. The residuals in this plot follow a normal distribution, as seen in the figure.

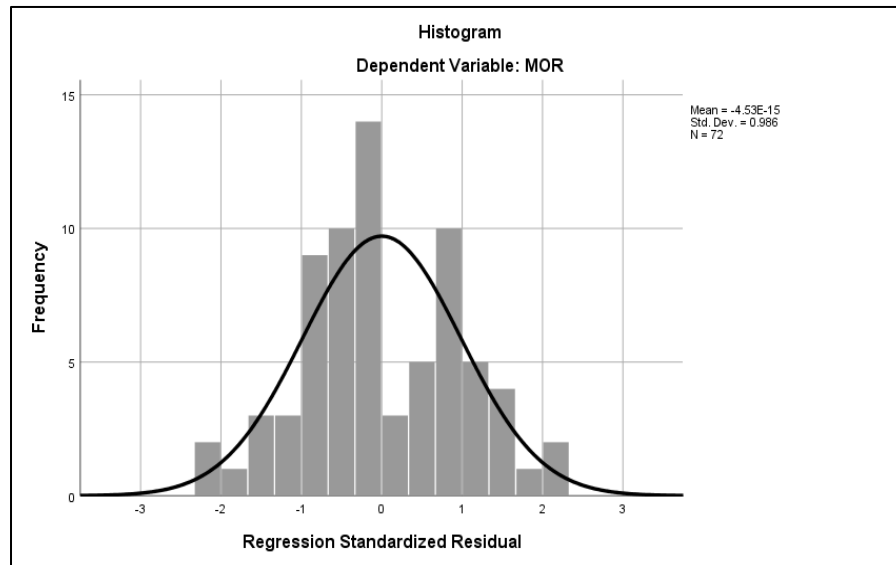


Figure 5-7: Standardized Residuals Histogram of flexural strength

Figure 5-8 depicts a normal probability plot of the residuals, which may be used to assess whether the residuals can be assumed to follow a normal distribution and, potentially, to identify outliers. Since the majority of residuals lie on a straight line in the normal probability plots of residuals shown in the preceding image, this proves that the residuals collected follow a normal distribution.

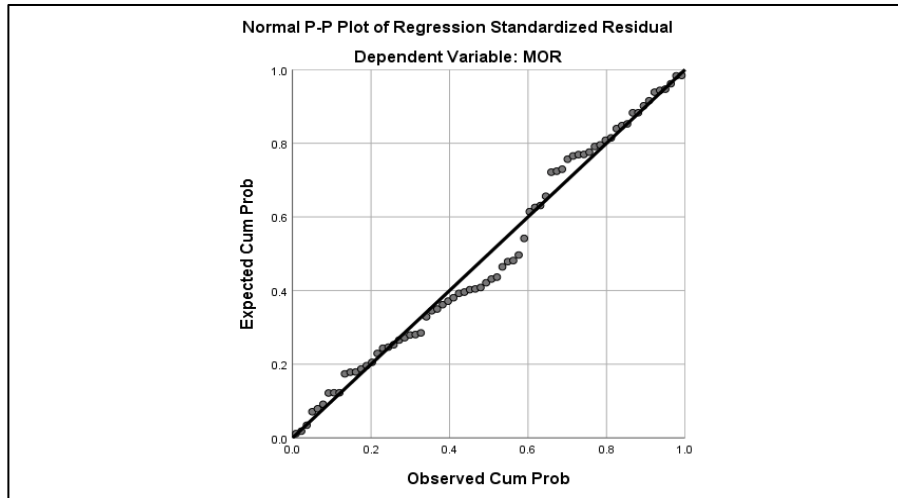


Figure 5-8: The Standardized Residual Normal P-P of flexural strength

Figure 5-9 displays graphs of the standardised residuals (errors) and predicted values of F.S, which may be used to test the homoscedasticity assumption. As seen in Figure 5-9, None of the residuals stands out significantly from the rest, and the pattern overall seems random. None of the residuals had Studentized values of three or less. There are also no out-of-the-ordinary residuals in this model.

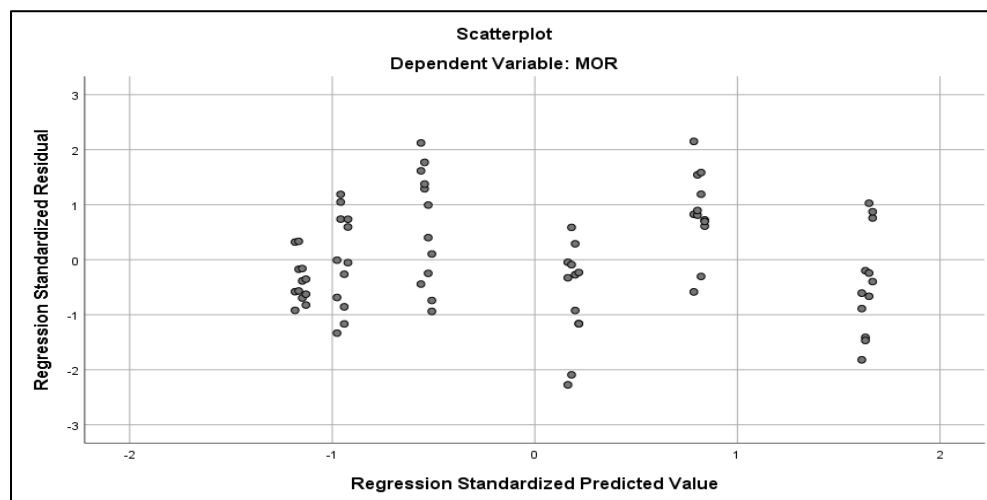


Figure 5-9: Scatter Plot of flexural strength

Chapter Six :Conclusions And Recommendations

6.1 Conclusions

This study examined the viability of using CDWTS ash as a partial binder replacement in cement-based grouts. The research was done on the fluidity, strength, and durability of CDWTS-infused cementitious grouts. Finally, the use of CDWTS as a partial replacement for conventional Portland cement (OPC) in grouting operations has the potential to increase the durability of grouts. The following inferences are made in light of the experimental studies:

- 1) The temperature of calcination effect upon the pozzolanic activity.
 - 2) From the chemical and physical properties, the CDWTS could be considered as SCM.
 - 3) A significant increase in compressive strength is seen throughout all curing ages for cement grout with CDWTS substituted; the optimal percent was 5%.
 - 4) Grouting with CDWTS improved the grout's integrity, as seen by the UPV readings of the grout prisms.
- Grout specimens with CDWTS absorbed less water than those with simply plain cement. Therefore, it is concluded that using CDWTS as a substitute in cement grouts improves the grout's durability.
 - Flexural strength showed slight increase with the replacement of CDWTS.
 - According to the result obtained from the microstructure SEM-EDS analysis there is considerable effect of CDWTS upon the hydration products. Where the replacement with 5% was the optimum enhancement, and that was consistent with the mechanical strength.

- The multiple regression models showed that the compressive and flexural strengths are not affected by the percentage of CDWTS added to the mixture

As a summary, in addition to lowering cement content, the use of CDWTS in cement grouts has been shown to increase the durability-related qualities of grout while not affecting the mechanical capabilities of grout compared to grout grouted with plain cement.

6.2 Recommendations for Further Work

Based on this research, the following recommendations are proposed:

- Investigate the possibility of using finer calcined CDWTS in concrete as the DTWS filled the small voids in the grout.
- It is also possible to test several samples from different water treatment plants and characterization the most important properties related to any other material such as (XRF, XRD, TG, FTIR, DLS) Tanique.
- Trying different temperature of calcination with various hour of duration.
- It possible to make binary or ternary mixture combination with CDWTS such as silica fume, glass powder and etc.
- Another treatment of DWTS can be made such as solidification.
- It is possible to try the difference between the raw DWTS and with treated for the cement composite.
- It is possible to replace the CDWTS as sand with the cement composite.

References

- ABDULREDHA, M., AL KHADDAR, R., JORDAN, D., KOT, P., ABDULRIDHA, A. & HASHIM, K. 2018. Estimating solid waste generation by hospitality industry during major festivals: A quantification model based on multiple regression. *Waste Management*, 77, 388-400.
- AHMAD, T., AHMAD, K. & ALAM, M. 2016a. Characterization of water treatment plant's sludge and its safe disposal options. *Procedia Environmental Sciences*, 35, 950-955.
- AHMAD, T., AHMAD, K. & ALAM, M. 2016b. Sustainable management of water treatment sludge through 3 'R' concept. *Journal of Cleaner Production*, 124, 1-13.
- AL-BUSALTAN, S. 2012. Development of new cold bituminous mixtures for road and highway pavements. School of Built Environment. PhD thesis Liverpool John Moores University, UK.
- ANDRADE, J. J. D. O., POSSAN, E., WENZEL, M. C. & SILVA, S. R. D. 2019. Feasibility of using calcined water treatment sludge in rendering mortars: A technical and sustainable approach. *Sustainability*, 11, 3576.
- ASTM C191 – 21. Standard Test Methods for Time of Setting of Hydraulic Cement by Vicat Needle¹.
- ASTM C597 – 16. Standard Test Method for Pulse Velocity Through Concrete¹.
- ASTM C618 – 22. Standard Specification for Coal Fly Ash and Raw or Calcined Natural Pozzolan for Use in Concrete¹.
- ASTM C109M – 21. Standard Test Method for Compressive Strength of Hydraulic Cement Mortars (Using 2-in. or [50-mm] Cube Specimens).
- ASTM C143M – 20. Standard Test Method for Slump of Hydraulic-Cement Concrete¹.
- ASTM C311M – 17. Standard Test Methods for Sampling and Testing Fly Ash or Natural Pozzolans for Use in Portland-Cement Concrete¹.
- ASTM C348 – 19. Standard Test Method for Flexural Strength of Hydraulic-Cement Mortars¹.
- ASTM C642-21. Standard Test Method for Density, Absorption, and Voids in Hardened Concrete¹. C642.
- ASTM C939-16. Standard Test Method for Flow of Grout for Preplaced-Aggregate Concrete (Flow Cone Method)¹.
- ASTM C942 – 10. Standard Test Method for Compressive Strength of Grouts for Preplaced-Aggregate Concrete in the Laboratory¹.
- ASTM C494, Standard Specification for Chemical Admixtures for Concrete, American Society of Testing and Materials, 2015.
- BABATUNDE, A. & ZHAO, Y. 2007. Constructive approaches toward water treatment works sludge management: an international review of beneficial reuses. *Critical Reviews in Environmental Science and Technology*, 37, 129-164.
- BELHAJ, D., ATHMOUNI, K., JERBI, B., KALLEL, M., AYADI, H. & ZHOU, J. L. 2016. Estrogenic compounds in Tunisian urban sewage treatment plant:

- occurrence, removal and ecotoxicological impact of sewage discharge and sludge disposal. *Ecotoxicology*, 25, 1849-1857.
- BONDAR, D., LYNDALE, C., MILESTONE, N., HASSANI, N. & RAMEZANIANPOUR, A. 2011. Effect of heat treatment on reactivity-strength of alkali-activated natural pozzolans. *Construction and Building Materials*, 25, 4065-4071.
- BONTON, A., BOUCHARD, C., BARBEAU, B. & JEDRZEJAK, S. 2012. Comparative life cycle assessment of water treatment plants. *Desalination*, 284, 42-54.
- CARDELL, C. & GUERRA, I. 2016. An overview of emerging hyphenated SEM-EDX and Raman spectroscopy systems: Applications in life, environmental and materials sciences. *TrAC Trends in Analytical Chemistry*, 77, 156-166.
- CELIK, F. & CANAKCI, H. 2015. An investigation of rheological properties of cement-based grout mixed with rice husk ash (RHA). *Construction and Building Materials*, 91, 187-194.
- CELIK, K., JACKSON, M. D., MANCIO, M., MERAL, C., EMWAS, A.-H., MEHTA, P. K. & MONTEIRO, P. J. 2014. High-volume natural volcanic pozzolan and limestone powder as partial replacements for portland cement in self-compacting and sustainable concrete. *Cement and concrete composites*, 45, 136-147.
- DASSANAYAKE, K., JAYASINGHE, G., SURAPANENI, A. & HETHERINGTON, C. 2015. A review on alum sludge reuse with special reference to agricultural applications and future challenges. *Waste Management*, 38, 321-335.
- DE AZEVEDO BASTO, P., JUNIOR, H. S. & DE MELO NETO, A. A. 2019. Characterization and pozzolanic properties of sewage sludge ashes (SSA) by electrical conductivity. *Cement and Concrete Composites*, 104, 103410.
- DE GODOY, L. G. G., ROHDEN, A. B., GARCEZ, M. R., DA COSTA, E. B., DA DALT, S. & DE OLIVEIRA ANDRADE, J. J. 2019. Valorization of water treatment sludge waste by application as supplementary cementitious material. *Construction and Building Materials*, 223, 939-950.
- DE GODOY, L. G. G., ROHDEN, A. B., GARCEZ, M. R., DA DALT, S. & GOMES, L. B. 2020. Production of supplementary cementitious material as a sustainable management strategy for water treatment sludge waste. *Case Studies in Construction Materials*, 12, e00329.
- DE OLIVEIRA ANDRADE, J. J., WENZEL, M. C., DA ROCHA, G. H. & DA SILVA, S. R. 2018. Performance of rendering mortars containing sludge from water treatment plants as fine recycled aggregate. *Journal of Cleaner Production*, 192, 159-168.
- DEMIRBOĞA, R., TÜRKMEN, İ. & KARAKOC, M. B. 2004. Relationship between ultrasonic velocity and compressive strength for high-volume mineral-admixed concrete. *Cement and concrete research*, 34, 2329-2336.
- DUAN, W., ZHUGE, Y., PHAM, P. N., WK CHOW, C., KEEGAN, A. & LIU, Y. 2020. Utilization of drinking water treatment sludge as cement replacement to mitigate alkali-silica reaction in cement composites. *Journal of Composites Science*, 4, 171.

- EMMELIN, A., BRANTBERGER, M., ERIKSSON, M., GUSTAFSON, G. & STILLE, H. 2007. Rock grouting. Current competence and development for the final repository.
- FRÍAS, M., DE LA VILLA, R. V., DE SOTO, I., GARCIA, R. & BALOA, T. 2014. Influence of activated drinking-water treatment waste on binary cement-based composite behavior: Characterization and properties. *Composites Part B: Engineering*, 60, 14-20.
- FRIAS, M., DE LA VILLA, R. V., GARCÍA, R., SÁNCHEZ DE ROJAS, M. I. & BALOA, T. A. 2013. Mineralogical evolution of kaolin-based drinking water treatment waste for use as pozzolanic material. The effect of activation temperature. *Journal of the American Ceramic Society*, 96, 3188-3195.
- GANAW, A. I. 2013. Rheology of grout for preplaced aggregate concrete. Investigation on the effect of different materials on the rheology of Portland cement based grouts and their role in the production of preplaced aggregate concrete. University of Bradford.
- GASTALDINI, A., HENGEN, M., GASTALDINI, M., DO AMARAL, F., ANTOLINI, M. & COLETTI, T. 2015. The use of water treatment plant sludge ash as a mineral addition. *Construction and building materials*, 94, 513-520.
- GOMES, S. D. C., ZHOU, J. L., LI, W. & LONG, G. 2019. Progress in manufacture and properties of construction materials incorporating water treatment sludge: A review. *Resources, conservation and recycling*, 145, 148-159.
- GONZÁLEZ, K. B., PACHECO, E., GUZMÁN, A., PEREIRA, Y. A., CUADRO, H. C. & VALENCIA, J. A. 2020. Use of sludge ash from drinking water treatment plant in hydraulic mortars. *Materials Today Communications*, 23, 100930.
- HABERT, G., CHOUPAY, N., MONTEL, J.-M., GUILLAUME, D. & ESCADEILLAS, G. 2008. Effects of the secondary minerals of the natural pozzolans on their pozzolanic activity. *Cement and Concrete Research*, 38, 963-975.
- HE, Z.-H., YANG, Y., YUAN, Q., SHI, J.-Y., LIU, B.-J., LIANG, C.-F. & DU, S.-G. 2021. Recycling hazardous water treatment sludge in cement-based construction materials: Mechanical properties, drying shrinkage, and nano-scale characteristics. *Journal of Cleaner Production*, 290, 125832.
- HEGAZY, B., FOUAD, H. A. & HASSANAIN, A. M. 2012. Brick manufacturing from water treatment sludge and rice husk ash. *Australian Journal of Basic and Applied Sciences*, 6, 453-461.
- HORPIBULSUK, S., SUKSIRIPATTANAPONG, C., SAMINGTHONG, W., RACHAN, R. & ARULRAJAH, A. 2016. Durability against wetting–drying cycles of water treatment sludge–fly ash geopolymer and water treatment sludge–cement and silty clay–cement systems. *Journal of Materials in Civil Engineering*, 28, 04015078.
- HUSSIN, M. W., KANG, L. S. & ZAKARIA, F. 2007. Engineering properties of high volume slag cement grout in tropical climate. *Malaysian journal of civil engineering*, 19.

- HWANG, C.-L. & HUYNH, T.-P. 2015. Evaluation of the performance and microstructure of ecofriendly construction bricks made with fly ash and residual rice husk ash. *Advances in Materials Science and Engineering*, 2015.
- INSTITUTE, A. C. ACI 232.2R-18. Report on the Use of Fly Ash in Concrete. ACI 232.2R-18.
- JAFER, H. M. 2017. Soft Soil Stabilisation Using a Novel Blended Cementitious Binder Produced from Waste Fly Ashes, Liverpool John Moores University (United Kingdom).
- JIA, Q., LU, J. & YANG, J. Investigation on the feasibility of resource utilizing drinking water treatment sludge as a pozzolan to prepare cement-based materials. *E3S Web of Conferences*, 2021. EDP Sciences, 02006.
- KEELEY, J., JARVIS, P. & JUDD, S. J. 2014. Coagulant recovery from water treatment residuals: a review of applicable technologies. *Critical Reviews in Environmental Science and Technology*, 44, 2675-2719.
- KERN, A. P., DIAS, M. F., KULAKOWSKI, M. P. & GOMES, L. P. 2015. Waste generated in high-rise buildings construction: A quantification model based on statistical multiple regression. *Waste Management*, 39, 35-44.
- KHADEMI, F. & JAMAL, S. M. 2017. Estimating the compressive strength of concrete using multiple linear regression and adaptive neuro-fuzzy inference system. *International Journal of Structural Engineering*, 8, 20-31.
- KWAN, A. & MCKINLEY, M. 2014. Effects of limestone fines on water film thickness, paste film thickness and performance of mortar. *Powder technology*, 261, 33-41.
- LAIDANI, Z. E.-A., BENABED, B., ABOUSNINA, R., GUEDDOUDA, M. K. & KHATIB, M. J. 2022. Potential pozzolanicity of Algerian calcined bentonite used as cement replacement: optimisation of calcination temperature and effect on strength of self-compacting mortars. *European Journal of Environmental and Civil Engineering*, 26, 1379-1401.
- LINKOV, P., ARTEMYEV, M., EFIMOV, A. E. & NABIEV, I. 2013. Comparative advantages and limitations of the basic metrology methods applied to the characterization of nanomaterials. *Nanoscale*, 5, 8781-8798.
- MAIDEN, P., HEARN, M., BOYSEN, R., CHIER, P., WARNECKE, M. & JACKSON, W. 2015. Alum sludge re-use, Investigation (10OS-42) prepared by GHD and Centre for Green Chemistry (Monash University) for the Smart Water Fund, Victoria, ACTEW Water & Seawater. Melbourne, Australia.
- MARTÍNEZ-GARCÍA, C., ELICHE-QUESADA, D., PÉREZ-VILLAREJO, L., IGLESIAS-GODINO, F. & CORPAS-IGLESIAS, F. 2012. Sludge valorization from wastewater treatment plant to its application on the ceramic industry. *Journal of environmental management*, 95, S343-S348.
- MERMERDAŞ, K., SÜLEYMAN, İ., SOR, N. H., MULAPEER, E. S. & EKMEKÇİ, Ş. 2020. The impact of artificial lightweight aggregate on the engineering features of geopolymer mortar. *Türk Doğa ve Fen Dergisi*, 9, 79-90.
- MOHAMMED, S. 2017. Processing, effect and reactivity assessment of artificial

- pozzolans obtained from clays and clay wastes: A review. *Construction and Building Materials*, 140, 10-19.
- NICHOLSON, P. G. 2014. *Soil improvement and ground modification methods*, Butterworth-Heinemann.
- O'KELLY, B. C. & QUILLE, M. E. 2010. Shear strength properties of water treatment residues. *Proceedings of the Institution of Civil Engineers-Geotechnical Engineering*, 163, 23-35.
- OWAID, H. M., HAMID, R. & TAHA, M. 2019. Durability properties of multiple-blended binder concretes incorporating thermally activated alum sludge ash. *Construction and Building Materials*, 200, 591-603.
- OYEDOTUN, T. D. T. 2018. X-ray fluorescence (XRF) in the investigation of the composition of earth materials: a review and an overview. *Geology, Ecology, and Landscapes*, 2, 148-154.
- PALLANT, J. 2020. *SPSS survival manual: A step by step guide to data analysis using IBM SPSS*, Routledge.
- PAPADAKIS, V. G. 1999. Effect of fly ash on Portland cement systems: Part I. Low-calcium fly ash. *Cement and concrete research*, 29, 1727-1736.
- PARIS, J. M., ROESSLER, J. G., FERRARO, C. C., DEFORD, H. D. & TOWNSEND, T. G. 2016. A review of waste products utilized as supplements to Portland cement in concrete. *Journal of Cleaner Production*, 121, 1-18.
- PHAM, P. N., DUAN, W., ZHUGE, Y., LIU, Y. & TORMO, I. E. S. 2021. Properties of mortar incorporating untreated and treated drinking water treatment sludge. *Construction and Building Materials*, 280, 122558.
- RAMIREZ, K. G., POSSAN, E., BITTENCOURT, P. R. S., CARNEIRO, C. & COLOMBO, M. 2018. Physico-chemical characterization of centrifuged sludge from the Tamanduá water treatment plant (Foz do Iguacu, PR). *Matéria (Rio de Janeiro)*, 23.
- ROSQUOËT, F., ALEXIS, A., KHELIDJ, A. & PHELIPOT, A. 2003. Experimental study of cement grout: Rheological behavior and sedimentation. *Cement and Concrete Research*, 33, 713-722.
- ŞAHMARAN, M., CHRISTIANTO, H. A. & YAMAN, İ. Ö. 2006. The effect of chemical admixtures and mineral additives on the properties of self-compacting mortars. *Cement and concrete composites*, 28, 432-440.
- SAHOO, S. & JHA, M. K. 2015. On the statistical forecasting of groundwater levels in unconfined aquifer systems. *Environmental earth sciences*, 73, 3119-3136.
- SAKIB, N., RAMAN, S. N., MUTALIB, A. A., JAMIL, M. & LOOI, D. T. 2020. Effects of supplementary cementitious materials on properties of cementitious grouts: A review.
- SALES, A., DE SOUZA, F. R. & ALMEIDA, F. D. C. R. 2011. Mechanical properties of concrete produced with a composite of water treatment sludge and sawdust. *Construction and Building Materials*, 25, 2793-2798.
- SENHADJI, Y., ESCADEILLAS, G., KHELAFI, H., MOULI, M. & BENOSMAN, A. S. 2012. Evaluation of natural pozzolan for use as supplementary cementitious material. *European Journal of Environmental and Civil Engineering*, 16, 77-96.

- SHAMAKI, M., ADU-AMANKWAH, S. & BLACK, L. 2021. Reuse of UK alum water treatment sludge in cement-based materials. *Construction and Building Materials*, 275, 122047.
- SIMONSEN, A. M. T., SOLISMAA, S., HANSEN, H. K. & JENSEN, P. E. 2020. Evaluation of mine tailings' potential as supplementary cementitious materials based on chemical, mineralogical and physical characteristics. *Waste Management*, 102, 710-721.
- STATISTICS, L. 2015. Binomial logistic regression using SPSS Statistics. *Statistical tutorials and software guides*.
- SUKSIRIPATTANAPONG, C., HORPIBULSUK, S., BOONGRASAN, S., UDOMCHAI, A., CHINKULKIJNIWAT, A. & ARULRAJAH, A. 2015. Unit weight, strength and microstructure of a water treatment sludge-fly ash lightweight cellular geopolymer. *Construction and Building Materials*, 94, 807-816.
- SUN, H., LI, Z., BAI, J., ALI MEMON, S., DONG, B., FANG, Y., XU, W. & XING, F. 2015. Properties of chemically combusted calcium carbide residue and its influence on cement properties. *Materials*, 8, 638-651.
- TABACHNICK, B. & FIDELL, L. 2013. *Using Multivariate Statistics*, 6th edn. (Pearson Education: Boston.).
- TAN, H., LIU, C., HUANG, Y. & GEUBELLE, P. 2005. The cohesive law for the particle/matrix interfaces in high explosives. *Journal of the Mechanics and Physics of Solids*, 53, 1892-1917.
- TAN, Ö. & ZAIMOGLU, A. S. 2004. Taguchi approach for investigation of the setting times on cement-based grouts.
- TANTAWY, M. 2015. Characterization and pozzolanic properties of calcined alum sludge. *Materials Research Bulletin*, 61, 415-421.
- THOMAS, M. 2013. *Supplementary Cementing Materials in Concrete*, 6000 Broken Sound Parkway NW, Suite 300 Boca Raton, FL 33487-2742, CRC Press.
- VANDEN HEEDE, P., RINGOOT, N., BEIRNAERT, A., VAN BRECHT, A., VAN DEN BRANDE, E., DE SCHUTTER, G. & DE BELIE, N. 2015. Sustainable high quality recycling of aggregates from waste-to-energy, treated in a wet bottom ash processing installation, for use in concrete products. *Materials*, 9, 9.
- WEI, L., ZHU, F., LI, Q., XUE, C., XIA, X., YU, H., ZHAO, Q., JIANG, J. & BAI, S. 2020. Development, current state and future trends of sludge management in China: Based on exploratory data and CO₂-equivalent emissions analysis. *Environment international*, 144, 106093.
- WILLIAMS, D. A., SAAK, A. W. & JENNINGS, H. M. 1999. The influence of mixing on the rheology of fresh cement paste. *Cement and concrete research*, 29, 1491-1496.
- YAGÜE, A., VALLS, S., VÁZQUEZ, E. & ALBAREDA, F. 2005. Durability of concrete with addition of dry sludge from waste water treatment plants. *Cement and Concrete Research*, 35, 1064-1073.
- YAHIA, A., TANIMURA, M. & SHIMOYAMA, Y. 2005. Rheological properties of highly flowable mortar containing limestone filler-effect of powder content and W/C ratio. *Cement and concrete Research*, 35, 532-539.
- YETGIN, Ş. & ÇAVDAR, A. 2006. Study of Effects of natural Pozzolan on Properties of Cement Mortars, *Journal of Materials in Civil Engineering*

الخلاصة

يستخدم الحقيين الأسمنتي على نطاق واسع لإعادة التأهيل الهيكلي للمكونات الخرسانية ، والخنادق ، وهبوط المناجم ، ومفاصل السدود ، وترميم مباني البناء ، والاستقرار الجيولوجي. لأن الطلب على صناعة الأسمنت ومواده يزداد كل عام ، مما يؤدي إلى انبعاث غاز ثاني أكسيد الكربون وزيادة استهلاك الطاقة ، من ناحية أخرى ، يزداد إنتاج مياه الشرب في محطة معالجة المياه بسبب زيادة عدد السكان؛ مما يؤدي بدوره إلى إنتاج النفايات وتدار هذه النفايات بشكل أساسي في مكب النفايات ، ونتيجة لذلك ، تستمر الجهود المبذولة لاستخدام المواد الإسمنتية التكميلية لتعزيز الخصائص الميكانيكية والاقتصادية والبيئية لمركبات الأسمنت. هذه الدراسة هي مثال فريد من نوعه يطور CDWTS المكلسن ليحل محل الأسمنت جزئياً في إنتاج الحقيين الاسمنتي.

بعد التحسين لكل من درجة حرارة الكلسنة والنعومة حيث تم اعتماد الدرجات (٧٠٠ درجة مئوية و ٥٠٠ ميكرومتر) لكل من درجة حرارة الكلسنة ودرجة النعومة على التوالي. تم تمييز الخصائص الكيميائية والفيزيائية (Strenght Activity Index(SAI)، X-Ray Florence (XRF) ، الوزن النوعي ، وحجم الجسيمات) لرماد CDWTS. تم استبدال رماد CDWTS بنسب (٠.٠٪ ، ٥٪ ، ١٠٪ ، ١٥٪) من وزن الأسمنت. ومع ذلك ، لتحديد تأثير CDWTS بشكل فردي على خصائص الحقيين ، يجب أن تظل كمية الماء والملدنات الفائقة ثابتة. تم إجراء العمل التجريبي في المختبر لتقدير الخصائص الجديدة بما في ذلك (وقت التماسك ، وقت الانسياب ، والهطول المصغر) ، والخصائص المتصلبة بما في ذلك (مقاومة الانضغاط ، مقاومة الانحناء ، سرعة الذبذبات فوق الصوتية ، الكثافة المتصلبة ، الفحص المجهر الإلكتروني - الأشعة السينية الوصفية للطاقة (SEM -EDAX) لحقيين الأسمنت المنتج. أوضحت النتائج أن الحقيين الأسمنتي الذي يحتوي على ٥٪ من CDWTS بديلاً عن الأسمنت كان له أفضل سلوك ويعتبر الأنسب للاستخدام . إلى جانب ذلك ، مع استبدال بنسبة ١٠٪ و ١٥٪ ، لوحظ أن الخواص الميكانيكية قد تقلصت بزيادة النسب المئوية ، لكنها تظل أعلى من المرجع. وفقاً لتحليل الحالة الجديد ، انخفضت قابلية تشغيل الحقيين الأسمنت بشكل كبير مع زيادة نسبة CDWTS. هذا يدل على أن CDWTS يمكن اعتباره بديلاً قابلاً للتطبيق للأسمنت البورتلاندي في المونة. كانت النتائج الميكانيكية متنسقة ومدعومة بتحليل SEM-EDX.

تم إجراء التحليل الإحصائي أيضاً باستخدام الإصدار ٢٦ من برنامج SPSS للتنبؤ بالخصائص المتصلبة (مقاومة الانضغاط ، مقاومة الانحناء ، و UPV) باستخدام الانحدار الخطي المتعدد (MLR). تم اعتبار نسب الخلط وعمر المعالجة كمتغيرات إدخال لنموذج MLR ، باستخدام طريقة الإدخال القياسية. تم تقييم أداء نماذج الانحدار هذه باستخدام معامل الارتباط المتعدد (R) ، ومضاعف R^2 ، ومعدل R^2 المعدل ، وإحصاء F ، والمستوى p ، والخطأ المعياري لتقدير إحصائيات ملائمة . تم حساب معاملات الانحدار لكل نموذج MLR باستخدام جميع المنهجيات. أظهرت نتائج النمذجة التي تم تحليلها أن نماذج MLR المستخدمة في هذه الدراسة فعالة في التنبؤ بسرعة الذبذبات فوق الصوتية ومقاومة الانحناء بدقة قياسية، حيث لم يتم تقدير مقاومة الانضغاط بكفاءة. بناءً على نتائج أطروحة العمل ، يمكن اعتبار CDWTS بديلاً قابلاً للتطبيق للإسمنت في إنتاج الحقن، مع استبدال يصل إلى ١٥٪.



جمهورية العراق
وزارة التعليم العالي و البحث العلمي
جامعة كربلاء
كلية الهندسة
قسم الهندسة المدنية

تخصيص مونة اسمنتية مستدامة لوحدات البنى التحتية

رسالة مقدمة الى مجلس كلية الهندسة / جامعة كربلاء وهي جزء من متطلبات نيل درجة الماجستير في
علوم الهندسة المدنية /البنى التحتية

من قبل:

هدى محمد حسن

بإشراف :

ا.م. أليث محمد رضا محمود

ا.م. د.محمد عبد الرزاق عبد الرضا